Two transmembrane transcriptional regulators coordinate to activate chitin-induced natural transformation in *Vibrio cholerae*

Allison C. Hullinger[1,†], Virginia E. Green[1,†], Catherine A. Klancher[1], Triana N. Dalia[1], and Ankur B. Dalia[1,*]

[1]Department of Biology, Indiana University, Bloomington, IN 47405.
[†]These authors contributed equally to this work.
*Corresponding author: ankdalia@iu.edu

ABSTRACT

Transcriptional regulators are a broad class of proteins that alter gene expression in response to environmental stimuli. Transmembrane transcriptional regulators (TTRs) are a subset of transcriptional regulators in bacteria that can directly regulate gene expression while remaining anchored in the membrane. Whether this constraint impacts the ability of TTRs to bind their DNA targets remains unclear. *Vibrio cholerae* uses two TTRs, ChiS and TfoS, to activate horizontal gene transfer by natural transformation in response to chitin by inducing the *tfoR* promoter (P_{tfoR}). While TfoS was previously shown to bind and regulate P_{tfoR} directly, the role of ChiS in P_{tfoR} activation remains unclear. Here, we show that ChiS directly binds P_{tfoR} upstream of TfoS, and that ChiS directly interacts with TfoS. By independently disrupting ChiS-P_{tfoR} and ChiS-TfoS interactions, we show that ChiS-P_{tfoR} interactions play the dominant role in P_{tfoR} activation. Correspondingly, we show that in the absence of ChiS, recruitment of the P_{tfoR} locus to the membrane is sufficient for P_{tfoR} activation when TfoS is expressed at native levels. Finally, we show that the overexpression of TfoS can bypass the need for ChiS for P_{tfoR} activation. All together, these data suggest a model whereby ChiS both (1) recruits the P_{tfoR} DNA locus to the membrane for TfoS and (2) directly interacts with TfoS, thereby recruiting it to the membrane-proximal promoter. This work furthers our understanding of the molecular mechanisms that drive chitin-induced responses in *V. cholerae* and more broadly highlights how the membrane-embedded localization of TTRs can impact their activity.

AUTHOR SUMMARY

Living organisms inhabit diverse environments where they encounter a wide range of stressors. To survive, they must rapidly sense and respond to their surroundings. One universally conserved mechanism to respond to stimuli is via the action of DNA-binding transcriptional regulators. In bacterial species, these regulators are canonically cytoplasmic proteins that freely diffuse within the cytoplasm. In contrast, an emerging class of transmembrane transcriptional regulators (TTRs) directly regulate gene expression from the cell membrane. Prior work shows that two TTRs, TfoS and ChiS, cooperate to activate horizontal gene transfer by natural transformation in response to chitin in the facultative pathogen *Vibrio cholerae*. However, how these TTRs coordinate to activate this response has remained unclear. Here, we show that ChiS likely promotes TfoS-dependent activation of natural transformation by (1) relocalizing its

target promoter to the membrane and (2) recruiting TfoS to the membrane proximal promoter through a direct interaction. Together, these results inform our understanding of both the *V. cholerae* chitin response and how TTR function can be impacted by their membrane localization.

INTRODUCTION

Bacterial species inhabit diverse environments where they encounter a wide range of stressors. To survive fluctuating conditions, they must have ways to sense and respond to environmental change. One such mechanism is the alteration of gene expression in response to specific environmental cues using a broad group of proteins called transcriptional regulators. Most commonly, transcriptional regulators are localized to the cytoplasm, where they can freely diffuse to find their DNA targets. However, recent work highlights the presence of transmembrane transcriptional regulators (TTRs) in diverse bacterial genomes [1]. In the few examples where they have been studied, TTRs were shown to bind to their DNA targets while remaining anchored in the membrane [2-7]. However, TTRs remain relatively poorly characterized, and the factors that influence how these proteins find their DNA targets to regulate gene expression remain unclear. Here, we investigate the mechanism of action for two chitin-responsive TTRs in *Vibrio cholerae*—TfoS and ChiS.

Natural transformation is a broadly conserved mode of horizontal gene transfer in which cells take up exogenous DNA to then integrate into their genome by homologous recombination. This process facilitates the rapid transfer of beneficial traits in diverse bacterial species. TfoS is a TTR that is required for the induction of natural transformation in *V. cholerae*. In addition to TfoS, induction of natural transformation requires chitin oligosaccharides, which *V. cholerae* liberates from the shells of crustacean zooplankton in the marine environment [8, 9]. Previous work shows that in the presence of chitin oligosaccharides, TfoS directly activates the expression of the small RNA (sRNA) *tfoR* by binding to its promoter (P_{tfoR}) [8, 9]. When transcribed, *tfoR* base pairs with the 5' untranslated region (UTR) of the mRNA of the master regulator of competence, TfoX, which allows for its translation [10]. TfoX then activates the expression of the genes necessary for DNA uptake and integration [11, 12]. Although this process requires chitin, it remains unclear whether TfoS senses chitin directly or indirectly through an intermediate.

ChiS is a TTR that is critical for induction of the chitin utilization program, a cascade of genes required for chitin uptake and catabolism that facilitates *V. cholerae* survival in marine habitats [13, 14]. When soluble chitin oligosaccharides enter the periplasm, they are bound by chitin-binding protein (CBP) [14, 15]. Chitin-bound CBP then activates ChiS, likely via a direct interaction [4]. Activated ChiS can then bind to the promoter of the chitobiose (*chb*) utilization operon (P_{chb}) to activate the expression of genes required for chitin uptake and catabolism [4, 14]. Like TfoS, ChiS is necessary for chitin-induced natural transformation [8, 9]. However, it is unclear whether this is due to its role in promoting chitin catabolism or whether it more directly regulates the genes required for natural transformation. Previous studies demonstrate that ChiS and TfoS are both required for chitin-induced P_{tfoR} activation, supporting the latter possibility [8, 9].

However, the mechanism by which ChiS and TfoS coordinate to regulate P_{tfoR} expression remains unclear.

RESULTS

ChiS binds to P_{tfoR} and is required for P_{tfoR} activation

Prior work suggests that ChiS and TfoS are both required for activation of P_{tfoR} [8, 9]. To formally test this, we generated strains with a chromosomally integrated P_{tfoR}-*gfp* transcriptional reporter. These strains also contained a previously described P_{chb}-*mCherry* construct [16], which serves as a reporter for ChiS activity. In addition, these strains contained a constitutively expressed [17] mTFP1 construct (P_{const2}-*mTFP1*), which was used to normalize for intrinsic noise in gene expression. All reporter constructs were chromosomally integrated at ectopic genomic sites. Because ChiS and TfoS are TTRs, the genomic locus where these transcriptional reporters are integrated could influence their activation (*i.e.*, they could be poorly activated if inserted into regions of the genome that are inaccessible to TTRs). It was therefore crucial to verify that these reporters could still be activated by their respective TTRs. When a strain harboring these constructs was incubated on chitin, we observed strong activation of both P_{tfoR} and P_{chb} by fluorescence microscopy (**Fig. 1A-C**). This result is consistent with their known regulation by chitin [4, 10], suggesting that these chromosomally integrated reporters are functional. Deleting either *chiS* or *tfoS* resulted in a complete loss of P_{tfoR} activation (**Fig. 1A-B**). Furthermore, we found that P_{chb} expression was completely ablated by Δ*chiS*, but not by Δ*tfoS* (**Fig. 1C**), which is consistent with the previously established role for ChiS in P_{chb} activation [4, 14]. These results confirm that both ChiS and TfoS are required for P_{tfoR} induction and demonstrate that these TTRs are not equally required for expression of all chitin-regulated promoters in *V. cholerae*. Furthermore, these results verify that the ectopic P_{tfoR} and P_{chb} reporter constructs can be activated by these TTRs.

The downstream consequence of P_{tfoR} induction is the expression of the genes necessary for horizontal gene transfer by natural transformation. We therefore also assessed the phenotypic impact of P_{tfoR} regulation by ChiS and TfoS on natural transformation. We found that deletion of either *chiS* or *tfoS* reduced natural transformation to the limit of detection (**Fig. 1D**), which is consistent with a critical role for both TTRs in inducing this behavior. Further, the overexpression of *tfoR*, which can induce competence in the absence of chitin [18-20], restores natural transformation in both Δ*chiS* and Δ*tfoS* backgrounds, suggesting that the inability of these strains to transform is due to the lack of *tfoR* expression (**Fig. S1**).

Our previous work has established that TfoS directly binds P_{tfoR} and that the ectopic expression of TfoS in the heterologous host *E. coli* is sufficient to drive P_{tfoR} induction even in the absence of ChiS [8]. However, our results above demonstrate that ChiS is still necessary for P_{tfoR} activation in *V. cholerae*. Thus, one possibility is that ChiS is necessary to stabilize natively expressed TfoS in *V. cholerae* (*i.e.,* that native TfoS is degraded in the absence of ChiS). To test this hypothesis, we generated a functional FLAG-tagged allele of TfoS (**Fig. S2**) and performed Western blot analysis. We found

140 that TfoS expression is not altered in the Δ*chiS* background (**Fig. S2C-D**). This result
141 suggests that ChiS does not promote P_{tfoR} activation by simply stabilizing TfoS.
142
143 Because ChiS does not stabilize TfoS, we reasoned that it may play a more active role
144 in regulating P_{tfoR}. Specifically, we hypothesized that ChiS may directly bind to P_{tfoR}. To
145 test this possibility, we performed chromatin immunoprecipitation-sequencing (ChIP-
146 seq) to identify ChiS binding sites *in vivo*. Consistent with our previous demonstrating
147 that ChiS binds to P_{chb} [4], we observed a strong ChIP peak at the P_{chb} promoter (**Fig.**
148 **1E**). ChIP peaks were also identified upstream of a predicted chitinase gene (VC2217)
149 as well as a putative glycosyltransferase (VC2487). Strikingly, this analysis also
150 revealed a strong ChIP peak at P_{tfoR} (**Fig. 1E**). To verify this result, we performed
151 electrophoretic mobility shift assays (EMSAs) using the purified cytoplasmic domain of
152 ChiS and found that it binds to P_{tfoR} *in vitro* (**Fig. 1F**). Furthermore, we show that this
153 interaction could be competitively inhibited by unlabeled P_{tfoR} probe but not by a
154 nonspecific promoter probe ($P_{VCA0053}$) (**Fig. 1F**), indicating that the interaction of ChiS
155 with P_{tfoR} is specific. Together, these results indicate that both ChiS and TfoS bind P_{tfoR},
156 and that both TTRs are critical for chitin-induced expression of TfoR.
157
158 ***ChiS directly interacts with TfoS***
159 Our results thus far are consistent with two possible models for activation of P_{tfoR} by
160 ChiS and TfoS. One possibility is that TfoS cannot bind P_{tfoR} independently, but instead
161 relies on ChiS binding at P_{tfoR} to recruit this DNA locus to the membrane so that it
162 becomes accessible to TfoS. Alternatively, ChiS may bind alongside TfoS at P_{tfoR} and
163 then directly interact with TfoS to allosterically regulate its activity by inducing a
164 conformational change that allows TfoS to bind P_{tfoR}. One of the primary differences
165 between these two models is that the latter has a strict requirement for a direct
166 interaction between ChiS and TfoS, while the former model does not.
167 To test whether ChiS and TfoS interact, we performed PopZ linked apical recruitment
168 (POLAR) assays [21]. In these assays, two putatively interacting proteins, the “bait” and
169 the “prey”, are translationally fused to distinct fluorescent markers to track their
170 independent localization. The bait protein is also fused to an H3H4 PopZ interaction
171 domain derived from *Caulobacter crescentus*. Upon induction of the polarly localizing
172 PopZ protein, the bait is relocalized to the cell pole. If the prey interacts with the bait, it
173 will also relocalize to the cell pole. If there is no interaction between the bait and prey,
174 the localization of the prey should be unaffected by PopZ induction. To assess
175 interactions between ChiS and TfoS, we generated strains expressing ChiS-msfGFP-
176 H3H4, TfoS-mCherry, and arabinose-inducible PopZ. In the absence of ChiS, TfoS-
177 mCherry was diffusely localized at the cell periphery, consistent with it being a
178 membrane-embedded regulator, and this localization did not change when PopZ was
179 induced (**Fig. 2**). We have previously found that ChiS-msfGFP-H3H4 inherently forms
180 foci at the cell periphery for reasons that remain unclear [4], and we have recapitulated
181 this observation here (**Fig. 2**). We found that in cells expressing both ChiS-msfGFP-
182 H3H4 and TfoS-mCherry, TfoS-mCherry forms foci that strongly colocalize with ChiS-
183 msfGFP-H3H4, suggesting that these proteins may interact (**Fig. 2**). Furthermore, when
184 PopZ is induced in these cells, both ChiS-msfGFP-H3H4 and TfoS-mCherry relocalize
185 to the cell poles, which is consistent with ChiS-TfoS interactions (**Fig. 2**). As an

186 independent way to assess ChiS-TfoS interactions, we also performed bacterial
187 adenylate cyclase two-hybrid (BACTH) assays [22]. Briefly, this assay involves
188 translationally fusing bait and prey proteins to each half of a split adenylate cyclase
189 reporter. Physical interaction between the bait and prey results in reconstitution of
190 adenylate cyclase activity, which induces beta-galactosidase expression in the *E. coli*
191 reporter strain. These BACTH assays also showed an interaction between ChiS and
192 TfoS, further suggesting that these proteins directly interact (**Fig. S3**).
193
194 ***ChiS-TfoS interactions support, but are not critical for P_{tfoR} activation***
195 We next wanted to test whether the interaction between ChiS and TfoS is critical for
196 P_{tfoR} activation, so we sought to disrupt the interaction between these proteins. To that
197 end, we created a functional chimera called Chi37, which is composed of the two
198 transmembrane domains and a truncated portion of the periplasmic domain of the
199 chemoreceptor Mlp37 translationally fused to the cytoplasmic domain of ChiS. Chi37 is
200 functional for P_{chb} activation and binds both P_{chb} and P_{tfoR} at wildtype levels *in vivo*
201 according to ChIP-qPCR assays (**Fig. S4**). However, POLAR assays demonstrate that
202 Chi37-msfGFP-H3H4 cannot relocalize TfoS-mCherry, indicating that Chi37-TfoS
203 interactions are below the limit of detection of this assay (**Fig. 2**). Because Chi37 retains
204 the ability to bind DNA but exhibits diminished interactions with TfoS, we used this allele
205 to test the impact of ChiS-TfoS interactions on P_{tfoR} activation.
206
207 If the interaction between ChiS and TfoS is essential for P_{tfoR} activation, we
208 hypothesized that a strain harboring Chi37 will not be able to activate P_{tfoR} expression,
209 and therefore will not allow for chitin-induced natural transformation. However, we found
210 that a Chi37 mutant had an intermediate phenotype – it exhibited decreased P_{tfoR}
211 activation and transformation compared to the parent, but this was still significantly
212 greater than Δ*chiS* (**Fig. 3B-D**). Because strains with Chi37 still retained the ability to
213 activate P_{tfoR} to some degree, it suggests that ChiS-TfoS interactions may not be strictly
214 required for allosteric regulation of TfoS activity. This result is also consistent with our
215 prior observation that TfoS can induce P_{tfoR} in *E. coli* even in the absence of ChiS [8].
216 However, these findings also make it clear that the interaction between ChiS and TfoS
217 is important for optimal P_{tfoR} induction.
218
219 ***Overexpression of TfoS bypasses the need for ChiS to activate P_{tfoR}***
220 Because ChiS-TfoS interactions contribute to optimal P_{tfoR} induction, we hypothesized
221 that this interaction might allow ChiS to recruit TfoS to the membrane-localized P_{tfoR}
222 DNA locus. Based on this model, we hypothesized that the overexpression of TfoS
223 within the cell should bypass the need for ChiS-TfoS interactions for optimal P_{tfoR}
224 activation. Under these conditions, we predicted that the likelihood of TfoS being
225 physically close to a membrane-proximal P_{tfoR} locus should be greatly increased,
226 thereby resulting in restoration of P_{tfoR} activation in the Chi37 background. To test this
227 hypothesis, we generated an IPTG-inducible TfoS construct (P_{tac}-*tfoS*) and confirmed
228 that this construct results in overexpression of TfoS via western blot analysis (**Fig. S2C-**
229 **D**).
230

231 Consistent with the proposed model, we found that overexpressing TfoS in the Chi37
232 background restored P_{tfoR} activation and natural transformation, suggesting that the
233 ChiS-TfoS interactions were no longer necessary due to the increased abundance of
234 TfoS in the cell (**Fig. 3B-D**). Furthermore, we found that overexpression of TfoS
235 overcomes the need for ChiS completely (*i.e.*, overexpression of TfoS recovers P_{tfoR}
236 induction and transformation in the Δ*chiS* background) (**Fig. 3B-D**). In contrast, the
237 overexpression of ChiS does not overcome the need for TfoS (**Fig. S5**). These results
238 suggest that the ChiS-dependent recruitment of P_{tfoR} to the membrane is only required
239 when TfoS is present at native levels; when TfoS is overexpressed, it obviates the need
240 for ChiS by increasing the likelihood that TfoS will come into contact with the P_{tfoR} DNA
241 locus (which will presumably be membrane-proximal at some frequency due to diffusion
242 of the DNA locus within the cell) independently.
243
244 ***The ChiS binding site in P_{tfoR} is critical for activation when TfoS is expressed at***
245 ***native levels***
246 Based on the model suggested above, we hypothesize that the ChiS binding site within
247 P_{tfoR} should be critical for activation when ChiS and TfoS are present at native levels.
248 Based on the sequence of the ChiS Binding Sites (CBS) in P_{chb} [4], a putative CBS
249 within P_{tfoR} was found at the 5' end of the promoter upstream of the TfoS binding site
250 (**Fig. 3A**). Indeed, truncating the 5' end of P_{tfoR} prevents ChiS binding (**Fig. S6**). We
251 refer to this truncated promoter construct as $P_{tfoR}^{\Delta CBS}$. The $P_{tfoR}^{\Delta CBS}$ mutation results in
252 minimal P_{tfoR} activation and inhibits chitin-induced natural transformation when ChiS and
253 TfoS were present at native levels (**Fig. 3B-D**).
254
255 Importantly, this strain still contains a functional copy of ChiS, but ChiS can no longer
256 bind at P_{tfoR}. If the loss of *tfoR* expression in $P_{tfoR}^{\Delta CBS}$ is due to a loss of ChiS-dependent
257 recruitment of P_{tfoR} to the membrane, we would predict that overexpression of TfoS
258 should bypass the impact of the $P_{tfoR}^{\Delta CBS}$ mutation (similar to what was observed in
259 Δ*chiS*). Indeed, we found that overexpression of TfoS recovers $P_{tfoR}^{\Delta CBS}$ induction and
260 natural transformation (**Fig. 3B-D**). This result also demonstrates that the truncation
261 used to generate $P_{tfoR}^{\Delta CBS}$ does not simply diminish the activity of this promoter.
262
263 In $P_{tfoR}^{\Delta CBS}$, ChiS binding is eliminated, preventing ChiS-dependent recruitment of the
264 promoter. Removing ChiS DNA recruitment allowed us to further isolate and test the
265 impact of ChiS-TfoS interactions. The ChiS in $P_{tfoR}^{\Delta CBS}$ can still bind to TfoS and other
266 DNA loci (*e.g.*, at P_{chb}), meaning that ChiS binding to TfoS should still be maintained in
267 this background. In contrast, Chi37 exhibits diminished interactions with TfoS in
268 $P_{tfoR}^{\Delta CBS}$ and therefore would likely exhibit greatly reduced allosteric activation. We
269 found that there was no increase in $P_{tfoR}^{\Delta CBS}$ activation when cells expressed ChiS vs
270 Chi37 (**Fig. 3B-C**). Consistent with this, neither ChiS or Chi37 is capable of supporting
271 chitin-induced natural transformation in the $P_{tfoR}^{\Delta CBS}$ background (**Fig. 3D**). These data
272 suggest that ChiS binding at P_{tfoR} likely plays a more important role in activation than its
273 interaction with TfoS.
274
275 ***Recruitment of P_{tfoR} to the membrane is sufficient for TfoS-dependent activation***

Together, our results suggest that ChiS binding at P_{tfoR} is more important than ChiS binding to TfoS for activation to occur. These data are consistent with two potential models. First, ChiS binding recruits P_{tfoR} to the membrane to make it accessible to TfoS. Alternatively, ChiS binding within P_{tfoR} may alter promoter architecture, which ultimately exposes the TfoS binding site. The distinction between these two models is that for the latter, there would likely be a requirement for native ChiS-CBS interactions within P_{tfoR} to alter promoter architecture. However, for the former model, we would predict that recruiting $P_{tfoR}^{\Delta CBS}$ to the membrane should be sufficient for activation. To test this hypothesis, we took advantage of the Tet repressor (TetR), which naturally binds its operator sequence, *tetO*, at high affinity. Specifically, we replaced the CBS within P_{tfoR} with *tetO* ($P_{tfoR}^{\Delta CBS::tetO}$) and swapped the native DNA-binding domain (DBD) of ChiS [23] for the full TetR protein (**Fig. 4A**). When we expressed $ChiS^{\Delta DBD}$-TetR in cells containing $P_{tfoR}^{\Delta CBS::tetO}$, we found that induction and natural transformation were partially recovered when compared to cells lacking the $ChiS^{\Delta DBD}$-TetR construct (**Fig. 4B-D**). To test this further, we incubated strains with anhydrotetracycline (ATc) to inhibit the DNA-binding activity of TetR. Under these conditions, both P_{tfoR} induction and natural transformation were ablated. This result is consistent with our hypothesis and suggests that recruitment of $P_{tfoR}^{\Delta CBS::tetO}$ to the membrane via $ChiS^{\Delta DBD}$-TetR binding is necessary for activation to occur (**Fig. 4B-D**). This result also argues against ChiS-dependent remodeling of *tfoR* promoter architecture, as native ChiS-CBS interactions have been entirely replaced by those of TetR and *tetO*. Importantly, overexpression of TfoS was able to rescue $P_{tfoR}^{\Delta CBS::tetO}$ induction even in the absence of ChiS, indicating that this promoter is fully functional (**Fig. 4B-D**).

If ChiS binding to P_{tfoR} primarily serves to recruit the promoter to the membrane, then we would hypothesize that the helical phasing of the CBS to the TfoS binding site (TBS) within P_{tfoR} is not critical for activation. To test this, we inserted either 5 bp (loss of phasing) or 10 bp (retains phasing) between the CBS and TBS in P_{tfoR} (**Fig. S7**). Inserting 5 bp, which disrupts phasing between the CBS and TBS, resulted in almost parent levels of P_{tfoR} activation. Similarly, insertion of 10 bp, which maintains phasing, resulted in full activation of P_{tfoR} (**Fig. S7**). Together, these results suggest that neither the phasing between the CBS and TBS nor the exact position of the CBS in P_{tfoR} is critical for activation. These results are consistent with a model in which ChiS binding to P_{tfoR} primarily serves to relocalize this promoter to the membrane.

DISCUSSION

In this study, we uncover how ChiS and TfoS coordinate to promote activation of natural transformation in *V. cholerae*. Specifically, our data are most consistent with a model wherein ChiS performs two functions to facilitate P_{tfoR} activation: (1) it recruits the P_{tfoR} DNA locus to the membrane and (2) it recruits TfoS to the membrane-proximal promoter through a direct interaction (**Fig. 5**).

The downstream effect of *tfoR* expression is the activation of the genes required for DNA uptake and integration by natural transformation. It is hypothesized that natural transformation is induced by chitin oligosaccharides because *Vibrio* species accumulate and form biofilms on chitinous surfaces in the aquatic environment. Thus, chitin is a

322 niche where diverse *Vibrios* are present, and represents an ideal site for genetic
323 exchange. In support of this model, prior work has uncovered that on chitin, *V. cholerae*
324 actively lyses neighboring bacteria to release their DNA as a substrate for natural
325 transformation [24, 25].
326
327 Our data suggests that simply overexpressing TfoS is sufficient to bypass the
328 requirement for ChiS for P_{tfoR} activation. ChiS and TfoS are likely independently
329 activated by chitin oligosaccharides [4, 8]. Why then has ChiS-dependent regulation of
330 P_{tfoR} been maintained in *V. cholerae*? One possibility is that this dual requirement
331 ensures that natural transformation is not induced until cells are experiencing conditions
332 where chitin oligosaccharides are abundant. This would prevent the inappropriate
333 expression of the large repertoire of genes required for natural transformation, which
334 might incur a significant fitness cost. This regulation is reminiscent of the “coincidence
335 detector” described for quorum sensing in *Vibrio* spp., which requires the simultaneous
336 detection of multiple autoinducers before activation can occur [26].
337
338 However, not all genes within the chitin regulon require the dual activity of ChiS and
339 TfoS. For example, the *chb* operon required for chitin uptake and catabolism is largely
340 dependent on ChiS alone as shown in this and prior work [4, 9]. Because nutrient
341 acquisition is likely a prerequisite for natural transformation, it is tempting to speculate
342 that the "relaxed” requirement for chitin-dependent induction of the *chb* operon is to
343 ensure that chitin uptake and catabolism is prioritized over genetic exchange by natural
344 transformation.
345
346 Here, we show that ChiS and TfoS are two TTRs that must cooperatively act to promote
347 P_{tfoR} activation. This cooperation between TTRs may be a common feature for this class
348 of transcriptional regulators. Indeed, *V. cholerae* contains another pair of TTRs, ToxRS
349 and TcpPH, that coordinate to activate the *toxT* promoter [5-7, 27, 28]. There are a
350 number of parallels between ToxRS/TcpPH dependent activation of P_{toxT} and ChiS/TfoS
351 dependent activation of P_{tfoR}. Namely, TcpPH is sufficient to activate P_{toxT} when
352 overexpressed, but requires ToxRS for P_{toxT} induction when expressed at native levels
353 [27]. Furthermore, the membrane-embedded localization of ToxRS is required for this
354 stimulatory activity [7, 28]. The ToxRS binding site in P_{toxT} is also located upstream of
355 the TcpPH binding site [7, 27]. These data are consistent with ToxRS facilitating
356 recruitment of P_{toxT} to the membrane for downstream binding and activation by TcpPH.
357 Recent results, however, suggest that ToxRS interactions with P_{toxT} may alter the
358 structure of the promoter to promote TcpPH-dependent activation [5, 6]. TcpPH and
359 ToxRS are members of a rapidly evolving family of signal transduction proteins in
360 enteric bacteria [29]. Thus, other members of this family may also coordinate to regulate
361 their downstream targets. One recent example is VrtAC, which likely coordinates with
362 VtrB to activate the expression and transertion of the type III secretion system in *V.*
363 *parahaemolyticus* [3]. Not all TTRs require cooperativity for their activity, however. This
364 is true for ChiS at the *chb* promoter [4, 9], ToxR at the *ompU* promoter [27], and *E. coli*
365 CadC at the *cadBA* operon [2].
366

The localization and diffusion of TTRs is clearly constrained compared to canonical cytoplasmic TRs. However, whether this constraint impacts how TTRs bind to their target sites is not clear. Our results suggest that natively expressed TfoS cannot activate P_{tfoR} unless ChiS is also present and able to bind P_{tfoR}. However, this requirement for ChiS can be overcome by simply overexpressing TfoS. This finding suggests that when natively expressed, TfoS cannot bind to P_{tfoR} in a manner that is sufficient to promote activation. Thus, the accessibility of the DNA binding targets for membrane-constrained TTRs may represent an additional layer of regulation that is a distinct property for this class of regulators when compared to canonical cytoplasmic transcriptional regulators. The DNA targets that TTRs bind must localize proximally to the membrane at some frequency. However, it is unclear if all regions of the genome are equally likely to diffuse and localize near the membrane in this manner. One possibility is that TTRs have evolved to bind to genomic loci that are more likely to come into contact with the membrane. Future work will focus on systematically assessing whether the constraint of membrane localization limits the genomic loci that TTRs can effectively bind and regulate.

Our data are consistent with a model in which membrane recruitment of P_{tfoR} is necessary for TfoS-dependent activation. This could be because TfoS, when expressed at native levels, lacks the ability to bind and recruit P_{tfoR} to the membrane by itself. However, the P_{tfoR} locus is not inherently difficult for a TTR to bind because we show that ChiS naturally binds to this locus from the membrane. Therefore, the P_{tfoR} DNA locus must come into contact with the membrane at some frequency. If so, one interpretation of our data is that TfoS is less capable of stably binding P_{tfoR} at the membrane compared to ChiS. Indeed, kinetic studies of the TTR CadC suggest that the mobility of the CadC protein within the membrane, but not the mobility of its DNA target, is rate-limiting for CadC-DNA interactions [30]. This finding indicates that some regions of the genome may contact the membrane with sufficient frequency that their diffusion / localization does not limit the TTR-DNA target search.

DNA-binding transcriptional regulators spend a large portion of their time transiently binding to DNA nonspecifically during their target search [31]. This transient binding can keep these proteins in close proximity to the nucleoid and help reduce the dimensionality of the 3D target search for a freely diffusing cytoplasmic DNA-binding protein. Therefore, a distinct possibility is that the membrane localization of TfoS does not make it more difficult for this regulator to bind to DNA. Instead, it could be that TfoS is capable of binding DNA, but does so with a relaxed specificity, which reduces the likelihood that it will identify and bind its sequence-specific target sites within the genome compared to other TTRs like ChiS. If so, ChiS binding at P_{tfoR} may simply “trap” this DNA locus at the membrane and help reduce the dimensionality of the target search for TfoS from a three-dimensional search into a two-dimensional search (due to the constrained diffusion of TfoS within a planar membrane). It is tempting to speculate that other molecular interactions, whether protein-protein or DNA-protein, also take advantage of the membrane as a planar space to increase the specificity and/or efficiency of the target search.

METHODS

Bacterial strains and culture conditions

All mutant strains were derived from the *Vibrio cholerae* El Tor strain E7946 [32]. Unless otherwise indicated, *V. cholerae* strains were grown in LB medium or on LB agar. When necessary, LB was supplemented with chloramphenicol (1 µg/mL), kanamycin (50 µg/mL), trimethoprim (10 µg/mL), spectinomycin (200 µg/mL), carbenicillin (100 µg/mL), erythromycin (10 µg/mL), zeocin (100 µg/mL), or sulfamethoxazole (100 µg/mL). A list of all strains used in this study can be found in **Table S1**.

Strain construction

Mutant constructs were made using splicing-by-overlap extension (SOE) PCR, as previously described [33]. Chromosomally integrated ectopic expression constructs were used throughout this study as previously described [34]. A list of all primers used to make mutant constructs can be found in **Table S2**. Mutant strains were generated by introducing constructs into strains by natural transformation; either chitin-induced natural transformation or chitin-independent natural transformation via the use of an IPTG-inducible *tfoX* plasmid (pMMB-*tfoX*) *[35].* The pMMB-*tfoX* plasmid was cured before strains were used in any experiments. Mutants were confirmed by PCR and/or sequencing.

Chitin-induced natural transformation assays

Strains were grown overnight in LB broth at 30°C rolling. Overnight cultures were then subcultured in LB broth, with 1 µM IPTG when applicable, and grown to mid-log phase (OD_{600} ~0.5-1.0). Cells were washed and resuspended in 0.5X Instant Ocean (IO; 7g/L, Aquarium Systems Inc.). Then, 1 mL chitin reactions were made by mixing 10^8 cells (suspending in 100 µL IO), 150 µL of chitin slurry (8g/150mL, Alfa Aesar), 750 µL IO, and 1 µM IPTG when applicable. Chitin reactions were incubated at 30°C static for ~18 hours. Next, 550 µL of supernatant was removed, and 500 ng of transforming DNA (tDNA) was mixed with the cells by inversion. The tDNA used replaced the frame-shifted transposase gene VC1807 (*i.e.*, a “neutral” gene locus) with either an Erm^R or Cm^R marker. A no tDNA control was included for each strain tested. Cells were incubated with DNA for 5 hours at 30°C static. Then, 500 µL LB broth was added to each reaction, and reactions were outgrown by shaking at 37°C for 2 hours. After outgrowth, reactions were plated for quantitative culture for total viable count (plated on plain LB agar) and transformants (plated on LB agar with antibiotic). Transformation frequency was calculated by dividing the CFU/mL of transformants by the CFU/mL of total viable counts.

Microscopy

Cells were imaged on an inverted Nikon Ti-2 microscope with a Plan Apo 60x objective lens, the appropriate filter cubes (FITC, YFP, mCherry, and/or CFP), a Hamamatsu ORCAFlash 4.0 camera, and Nikon NIS Elements imaging software. Image analysis was conducted using the MicrobeJ plugin [36] in Fiji [37]. Cell body segmentation was performed using the “medial axis” mode on the phase image. Segmentation parameters were adjusted for each image, but generally fell within the following ranges: minimum

area of 0.45 μm^2, length between 0.6-2.7 μm, and width between 0.3-1 μm. Fluorescence was measured in the interior of segmented cells, which included the cell periphery and cytoplasm.

PopZ-linked apical recruitment (POLAR) assays

Strains were grown overnight in LB broth at 30°C rolling and were supplemented with 10 μM IPTG to induce *P_{tac}-tfoS-mCherry, P_{tac}-chiS-GFP-H3H4, and/or P_{tac}-chi37-GFP-H3H4* constructs. For POLAR experiments, LB broth was also supplemented with 0.05% arabinose to induce *P_{bad}-PopZ* expression. For efficient polar relocalization and to avoid issues with cell curvature, the curvature determinant *crvA* [38] was deleted in all colocalization strains. Overnight cultures were washed and resuspended in 0.5X IO. Cells were then placed on a glass coverslip beneath a 0.4% IO gelzan pad and imaged using FITC and mCherry filter cubes. Heat maps were generated by analyzing the fluorescence localization of 300 cells per replicate. To quantify polar localization, the distance of fluorescence to the nearest cell pole was measured in each channel. Fluorescence within 0.2 μm of the cell pole was conservatively denoted as polarly localized.

Bacterial adenylate cyclase two-hybrid assays

ChiS and TfoS genes were amplified using PCR and cloned into the BACTH vectors pKT25, pUT18C, pKNT25, and pUT18 to generate N- and C-terminal fusions to the T18 and T25 fragments of adenylate cyclase. Miniprepped plasmids were then cotransformed into *E. coli* BTH101. Transformations were plated onto LB agar plates with kanamycin (50 μg/mL) and carbenicillin (100 μg/mL) to select for transformants that received both plasmids. The resulting strains were then grown up overnight in LB broth at 30°C, and 3 μL of the overnight culture was spotted onto an LB agar plate supplemented with 500 μM IPTG, kanamycin (50 μg/mL), carbenicillin (100 μg/mL), and 5-bromo-4-chloro-3-indolyl-β-d-galactopyranoside (X-gal) (40 μg/mL). Plates were incubated at 30°C for 48 hours before imaging on an HP Scanjet G4010 flatbed scanner.

Electrophoretic mobility shift assays (EMSAs)

Binding reactions contained 10 mM Tris·HCl pH 7.5, 1 mM EDTA, 10 mM KCl, 1 mM DTT, 50 μg/mL BSA, 0.1 mg/mL salmon sperm DNA, 5% glycerol, 3 nM DNA probe, and purified MBP-ChiS cytoplasmic domain [4] at 25 nM, 50 nM, 100 nM, 200 nM, 400 nM, and 800 nM concentrations (diluted in 10 mM Tris pH 7.5, 10 mM KCl, 1 mM DTT, and 5% glycerol). Binding reactions were incubated in the dark at room temperature for 20 minutes before being loaded into a 0.5X Tris Borate EDTA (TBE) polyacrylamide gel. Gels were run in 0.5X TBE buffer at 4°C, then imaged for Cy5 fluorescence on a ProteinSimple FluorChem R system.

Cy5-labeled DNA probes were made by Taq PCR with 4.34 μM Cy5-dCTP. Unlabeled probes were made by Phusion PCR.

Fluorescence reporter assays

Strains were grown overnight in LB broth, supplemented with 1 μM IPTG and/or 50 ng/mL ATc when applicable, at 30°C rolling. Then, overnight cultures were washed and

505 resuspended in IO. 1 mL chitin reactions were made by mixing 10^8 cells (suspended in
506 100 µL IO), 150 µL of chitin slurry (8g/150mL), 750 µL IO, and 1 µM IPTG and/or 50
507 ng/mL ATc when applicable. Chitin reactions were incubated at 30°C shaking for 24
508 hours. Next, reactions were vortexed to dislodge the cells from the chitin. The
509 supernatants (containing the resuspended cells) were then centrifuged, resuspended in
510 IO, and placed on a glass coverslip beneath a 0.2% IO gelzan pad. Cells were then
511 imaged using mCherry, YFP, and CFP filter cubes. Image analysis was performed to
512 quantify the average fluorescence per cell in each channel. The background
513 fluorescence was determined in each channel by imaging and analyzing a non-
514 fluorescent strain, which was then subtracted from all samples. Reporter fluorescence
515 (GFP or mCherry) was then divided by the fluorescence of the CFP channel to
516 normalize against the constitutively expressed mTFP1 construct. The geometric mean
517 was then calculated from 300 individual cells for each replicate.
518
519 **Western blotting**
520 Strains were grown overnight in LB broth, supplemented with 1 µM IPTG when
521 applicable, at 30°C rolling. Overnight cultures were then washed and resuspended to
522 OD_{600}=100 in IO. Cells were then mixed 1:1 with 2X SDS-PAGE sample buffer (200 mM
523 Tris pH 6.8, 25% glycerol, 4.1% SDS, 0.02% Bromophenol Blue, 5% β-
524 mercaptoethanol) and boiled for 10 minutes. To blot for TfoS-FLAG, 4 µL of each
525 sample was separated on a 15% SDS-PAGE gel. To blot for RpoA, 2 µL of each sample
526 was separated on a 15% SDS-PAGE gel. Following SDS-PAGE, the proteins were
527 transferred to a polyvinylidene difluoride (PVDF) membrane by electrophoresis, and
528 then membranes were blocked for 1 hour in 2% milk. Next, membranes were incubated
529 rocking at room temperature overnight with primary antibody: rabbit polyclonal anti-
530 FLAG (Sigma) or mouse monoclonal anti-RpoA (Biolegend). Membranes were then
531 washed and incubated with either anti-mouse or anti-rabbit horseradish peroxidase-
532 conjugated secondary antibody for three hours rocking at room temperature. Then, blots
533 were washed, developed with Pierce ECL Western blotting substrate, and imaged with
534 a ProteinSimple FluorChem R system.
535
536 **Chromatin immunoprecipitation assays**
537 Chromatin Immunoprecipitation (ChIP) assays were performed exactly as previously
538 described [39]. *V. cholerae* strains were initiated from freezer stocks and incubated at
539 30°C in LB broth rolling for ~16 hours. The following day, cultures were subcultured into
540 fresh LB to an OD_{600} of 0.08 and incubated rolling for 6 hours at 30°C. Cells were
541 incubated with 1% paraformaldehyde at room temperature for 20 minutes shaking to
542 crosslink DNA and proteins. A 1.2 molar excess of Tris (10 minutes, room temperature,
543 shaking) was used to quench residual paraformaldehyde. Crosslinked cells were
544 washed twice with TBS (25 mM Tris HCl, pH 7.5 and 125 mM NaCl) and then frozen at -
545 80°C. Cells were then resuspended in lysis buffer (1x FastBreak cell lysis reagent
546 (Promega), 50 µg/mL lysozyme, 1% Triton X-100, 1 mM PMSF, and 1x protease
547 inhibitor cocktail; 100x inhibitor cocktail contained the following: 0.07 mg/mL
548 phosphoramidon (Santa Cruz), 0.006 mg/mL bestatin (MPbiomedicals/Fisher Scientific),
549 1.67 mg/mL AEBSF (Gold Bio), 0.07 mg/mL pepstatin A (DOT Scientific), 0.07 mg/mL
550 E64 (Gold Bio) suspended in DMSO) to an OD_{600} of 50.0. These resuspensions were

551 incubated rocking at room temperature for 20 minutes to permit cell lysis. Lysates were
552 then sonicated to shear DNA into 200-300bp fragments (sonication was performed with
553 a Fisherbrand Model 705 Sonic Dismembrator 6 times for 10 seconds at 1% amplitude,
554 resting on ice for at least 30 seconds between each sonication). The sonicated lysates
555 were then clarified by centrifugation and diluted 1:5 in Immunoprecipitation (IP) Buffer
556 (50 mM HEPES NaOH pH 7.5, 150 mM NaCl, 1 mM EDTA, and 1% Triton X-100). An
557 "input DNA" sample was collected from this diluted lysate. 1 mL of this diluted lysate
558 was then added to Pierce anti-DYKDDDDK magnetic agarose equilibrated in IP buffer
559 and then incubated at room temperature with end-over-end mixing. After two hours of
560 incubation, a magnetic separation rack was used to facilitate removal of the
561 supernatant. The agarose was washed twice with IP Buffer for 1 minute, once with
562 Wash Buffer 1 (50 mM HEPES NaOH pH 7.5, 1 mM EDTA, 1% Triton X-100, 500 mM
563 NaCl, and 0.1% SDS) for 5 minutes, once with Wash Buffer 2 (10 mM Tris HCl pH 8.0,
564 250 mM LiCl, 1 mM EDTA, 0.5% NP- 40, and 1% Triton X-100) for 5 minutes, and once
565 with Buffer TE (10 mM tris pH 8.0 and 1 mM EDTA) for 1 minute. SDS elution buffer (50
566 mM Tris HCl pH 7.5, 10 mM EDTA, and 1% SDS) was used to elute protein and DNA
567 off the magnetic agarose (30 minutes at 65°C). Supernatant was collected and digested
568 for 2 hours with 20 µg Proteinase K in SDS Elution Buffer at 42°C. 6 hours of incubation
569 at 65°C was then used to reverse crosslinking. Both the input and the output samples
570 were then purified to remove non-DNA components. The abundance of P_{tfoR} in the input
571 DNA (diluted 1:100) and output DNA was then quantified using quantitative PCR with
572 iTaq Universal SYBR Green Supermix (Bio-Rad). A fold enrichment value was then
573 generated by measuring the abundance of the *tfoR* promoter in the output (following
574 immunoprecipitation) relative to the input (prior to immunoprecipitation). A locus that is
575 not bound by ChiS or TfoS (*rpoB*) was used to normalize for total amount of DNA in the
576 sample.
577
578 **ChIP-seq assays**
579 ChIP input and output DNA were prepared exactly as described in "Chromatin
580 immunoprecipitation assays" above. Sequencing libraries were prepared using the
581 NEBNext Ultra II DNA Library Prep Kit (New England Biolabs) for Illumina according to
582 manufacturer's instructions. Libraries were then analyzed on a 4200 TapeStation
583 (Agilent), pooled, and then loaded on a NextSeq 1000/2000 P2 Reagents (100 Cycles)
584 v3 flow cell configured to generate 2 x 61 nt paired-end reads. Demultiplexing was
585 performed with bcl2fastq, version 2.20.0.
586
587 Reads were then analyzed using the open-source web-based Galaxy server [40].
588 Demultiplexed paired-end fastq files were aligned to the *V. cholerae* genome (*Vibrio*
589 *cholerae* O1 biovar El Tor str. N16961, NCBI RefSeq assembly: GCF_000006745.1)
590 using bowtie2 with default parameters for paired-end data. Output BAM files were
591 converted to bigWig files for peak visualization using bamCoverage. Bin size was set to
592 50 bp and coverage was normalized to 1x. Effective genome size was user-specified at
593 4,033,464. The tool bigwigCompare was then used to visualize the enrichment of output
594 over input bigWig files. The ChIP output file was set as the "treatment file" and the ChIP
595 input was set as the "bigwig file" and the option "compute the ratio signals" was used to
596 generate plots for of the ChIP ratio. To account for regions of zero coverage, a

pseudocount of 0.01 was added to each binned region. The output bigWig file was then visualized on Integrated Genome Viewer 2.8.4. Raw and processed data were uploaded to NCBI GEO (Accession: GSE284091).

Statistical Comparisons

All statistical comparisons were made in Graphpad Prism and the statistical tests used are indicated in figure legends. For summary statistics and a complete list of all statistical comparisons, see **S1 Dataset**.

ACKNOWLEDGEMENTS

We would like to thank the Center for Genomics and Bioinformatics at Indiana University for assistance with ChIP-seq library prep and sequencing. We would also like to thank Gabe Zentner for his assistance and advice on ChIP-seq analysis. This work was supported by grant R35GM128674 from the National Institutes of Health to ABD.

REFERENCES

1. Demey LM, Gumerov VM, Xing J, Zhulin IB, DiRita VJ. Transmembrane Transcription Regulators Are Widespread in Bacteria and Archaea. Microbiol Spectr. 2023;11(3):e0026623. Epub 20230508. doi: 10.1128/spectrum.00266-23. PubMed PMID: 37154724; PubMed Central PMCID: PMCPMC10269533.

2. Brameyer S, Rösch TC, El Andari J, Hoyer E, Schwarz J, Graumann PL, Jung K. DNA-binding directs the localization of a membrane-integrated receptor of the ToxR family. Commun Biol. 2019;2:4. Epub 20190104. doi: 10.1038/s42003-018-0248-7. PubMed PMID: 30740540; PubMed Central PMCID: PMCPMC6320335.

3. Kaval KG, Chimalapati S, Siegel SD, Garcia N, Jaishankar J, Dalia AB, Orth K. Membrane-localized expression, production and assembly of Vibrio parahaemolyticus T3SS2 provides evidence for transertion. Nat Commun. 2023;14(1):1178. Epub 20230302. doi: 10.1038/s41467-023-36762-z. PubMed PMID: 36859532; PubMed Central PMCID: PMCPMC9977878.

4. Klancher CA, Yamamoto S, Dalia TN, Dalia AB. ChiS is a noncanonical DNA-binding hybrid sensor kinase that directly regulates the chitin utilization program in Vibrio cholerae. Proceedings of the National Academy of Sciences. 2020;117(33):20180-9. doi: 10.1073/pnas.2001768117.

5. Haas BL, Matson JS, DiRita VJ, Biteen JS. Single-molecule tracking in live Vibrio cholerae reveals that ToxR recruits the membrane-bound virulence regulator TcpP to the toxT promoter. Mol Microbiol. 2015;96(1):4-13. Epub 20141104. doi: 10.1111/mmi.12834. PubMed PMID: 25318589; PubMed Central PMCID: PMCPMC6025817.

6. Calkins AL, Demey LM, Karslake JD, Donarski ED, Biteen JS, DiRita VJ. Independent Promoter Recognition by TcpP Precedes Cooperative Promoter Activation by TcpP and ToxR. mBio. 2021;12(5):e0221321. Epub 20210907. doi: 10.1128/mBio.02213-21. PubMed PMID: 34488449; PubMed Central PMCID: PMCPMC8546550.

7. Canals A, Pieretti S, Muriel-Masanes M, El Yaman N, Plecha SC, Thomson JJ, et al. ToxR activates the Vibrio cholerae virulence genes by tethering DNA to the membrane through versatile binding to multiple sites. Proc Natl Acad Sci U S A. 2023;120(29):e2304378120. Epub 20230710. doi: 10.1073/pnas.2304378120. PubMed PMID: 37428913; PubMed Central PMCID: PMCPMC10629549.

8. Dalia Ankur B, Lazinski David W, Camilli A. Identification of a Membrane-Bound Transcriptional Regulator That Links Chitin and Natural Competence in Vibrio cholerae. mBio. 2014;5(1):10.1128/mbio.01028-13. doi: 10.1128/mbio.01028-13.

9. Yamamoto S, Mitobe J, Ishikawa T, Wai SN, Ohnishi M, Watanabe H, Izumiya H. Regulation of natural competence by the orphan two-component system sensor kinase ChiS involves a non-canonical transmembrane regulator in Vibrio cholerae. Molecular Microbiology. 2014;91(2):326-47. doi: https://doi.org/10.1111/mmi.12462.

10. Yamamoto S, Izumiya H, Mitobe J, Morita M, Arakawa E, Ohnishi M, Watanabe H. Identification of a chitin-induced small RNA that regulates translation of the tfoX gene, encoding a positive regulator of natural competence in Vibrio cholerae. J Bacteriol. 2011;193(8):1953-65. Epub 2011/02/15. doi: JB.01340-10 [pii]

10.1128/JB.01340-10. PubMed PMID: 21317321; PubMed Central PMCID: PMC3133033.

11. Lo Scrudato M, Blokesch M. The regulatory network of natural competence and transformation of Vibrio cholerae. PLoS Genet. 2012;8(6):e1002778. Epub 2012/06/28. doi: 10.1371/journal.pgen.1002778

PGENETICS-D-12-00108 [pii]. PubMed PMID: 22737089; PubMed Central PMCID: PMC3380833.

12. Seitz P, Blokesch M. DNA-uptake machinery of naturally competent Vibrio cholerae. Proc Natl Acad Sci U S A. 2013;110(44):17987-92. Epub 2013/10/16. doi: 1315647110 [pii]

10.1073/pnas.1315647110. PubMed PMID: 24127573.

13. Li X, Roseman S. The chitinolytic cascade in Vibrios is regulated by chitin oligosaccharides and a two-component chitin catabolic sensor/kinase. Proc Natl Acad Sci U S A. 2004;101(2):627-31. Epub 2003/12/31. doi: 10.1073/pnas.0307645100

0307645100 [pii]. PubMed PMID: 14699052; PubMed Central PMCID: PMC327198.

14. Meibom KL, Li XB, Nielsen AT, Wu CY, Roseman S, Schoolnik GK. The Vibrio cholerae chitin utilization program. Proc Natl Acad Sci U S A. 2004;101(8):2524-9. Epub 2004/02/26. doi: 101/8/2524 [pii]. PubMed PMID: 14983042; PubMed Central PMCID: PMC356983.

15. Kitaoku Y, Fukamizo T, Kumsaoad S, Ubonbal P, Robinson RC, Suginta W. A structural model for (GlcNAc)(2) translocation via a periplasmic chitooligosaccharide-binding protein from

686 marine Vibrio bacteria. J Biol Chem. 2021;297(3):101071. Epub 20210813. doi:
687 10.1016/j.jbc.2021.101071. PubMed PMID: 34400168; PubMed Central PMCID:
688 PMCPMC8449061.

689
690 16. Klancher CA, Hayes CA, Dalia AB. The nucleoid occlusion protein SlmA is a direct
691 transcriptional activator of chitobiose utilization in Vibrio cholerae. PLoS Genet.
692 2017;13(7):e1006877. doi: 10.1371/journal.pgen.1006877. PubMed PMID: 28683122; PubMed
693 Central PMCID: PMCPMC5519180.

694
695 17. Davis JH, Rubin AJ, Sauer RT. Design, construction and characterization of a set of
696 insulated bacterial promoters. Nucleic Acids Res. 2011;39(3):1131-41. Epub 20100915. doi:
697 10.1093/nar/gkq810. PubMed PMID: 20843779; PubMed Central PMCID: PMCPMC3035448.

698
699 18. Ellison CK, Dalia TN, Vidal Ceballos A, Wang JC, Biais N, Brun YV, Dalia AB. Retraction of
700 DNA-bound type IV competence pili initiates DNA uptake during natural transformation in Vibrio
701 cholerae. Nat Microbiol. 2018;3(7):773-80. doi: 10.1038/s41564-018-0174-y. PubMed PMID:
702 29891864.

703
704 19. Meibom KL, Blokesch M, Dolganov NA, Wu CY, Schoolnik GK. Chitin induces natural
705 competence in Vibrio cholerae. Science. 2005;310(5755):1824-7. Epub 2005/12/17. doi:
706 310/5755/1824 [pii]

707 10.1126/science.1120096. PubMed PMID: 16357262.

708
709 20. Dalia AB. RpoS is required for natural transformation of Vibrio cholerae through regulation of
710 chitinases. Environ Microbiol. 2016;18(11):3758-67. doi: 10.1111/1462-2920.13302. PubMed
711 PMID: 26999629.

712
713 21. Lim HC, Bernhardt TG. A PopZ-linked apical recruitment assay for studying protein-protein
714 interactions in the bacterial cell envelope. Mol Microbiol. 2019;112(6):1757-68. Epub
715 2019/09/25. doi: 10.1111/mmi.14391. PubMed PMID: 31550057; PubMed Central PMCID:
716 PMCPMC7218919.

717
718 22. Karimova G, Pidoux J, Ullmann A, Ladant D. A bacterial two-hybrid system based on a
719 reconstituted signal transduction pathway. Proc Natl Acad Sci U S A. 1998;95(10):5752-6. Epub
720 1998/05/20. doi. PubMed PMID: 9576956; PubMed Central PMCID: PMCPMC20451.

721
722 23. Klancher CA, Minasov G, Podicheti R, Rusch DB, Dalia TN, Satchell KJF, et al. The ChiS-
723 Family DNA-Binding Domain Contains a Cryptic Helix-Turn-Helix Variant. mBio. 2021;12(2).
724 Epub 2021/03/18. doi: 10.1128/mBio.03287-20. PubMed PMID: 33727356; PubMed Central
725 PMCID: PMCPMC8092284.

726
727 24. Borgeaud S, Metzger LC, Scrignari T, Blokesch M. The type VI secretion system of Vibrio
728 cholerae fosters horizontal gene transfer. Science. 2015;347(6217):63-7. doi:
729 10.1126/science.1260064. PubMed PMID: 25554784.

25. Molina-Quiroz RC, Dalia TN, Camilli A, Dalia AB, Silva-Valenzuela CA. Prophage-Dependent Neighbor Predation Fosters Horizontal Gene Transfer by Natural Transformation. mSphere. 2020;5(6). Epub 2020/11/13. doi: 10.1128/mSphere.00975-20. PubMed PMID: 33177216; PubMed Central PMCID: PMCPMC7657591.

26. Mok KC, Wingreen NS, Bassler BL. Vibrio harveyi quorum sensing: a coincidence detector for two autoinducers controls gene expression. EMBO J. 2003;22(4):870-81. doi: 10.1093/emboj/cdg085. PubMed PMID: 12574123; PubMed Central PMCID: PMCPMC145445.

27. Krukonis ES, Yu RR, Dirita VJ. The Vibrio cholerae ToxR/TcpP/ToxT virulence cascade: distinct roles for two membrane-localized transcriptional activators on a single promoter. Mol Microbiol. 2000;38(1):67-84. doi: 10.1046/j.1365-2958.2000.02111.x. PubMed PMID: 11029691.

28. Crawford JA, Krukonis ES, DiRita VJ. Membrane localization of the ToxR winged-helix domain is required for TcpP-mediated virulence gene activation in Vibrio cholerae. Mol Microbiol. 2003;47(5):1459-73. doi: 10.1046/j.1365-2958.2003.03398.x. PubMed PMID: 12603748.

29. Kinch LN, Cong Q, Jaishankar J, Orth K. Co-component signal transduction systems: Fast-evolving virulence regulation cassettes discovered in enteric bacteria. Proc Natl Acad Sci U S A. 2022;119(24):e2203176119. Epub 2022/06/02. doi: 10.1073/pnas.2203176119. PubMed PMID: 35648808; PubMed Central PMCID: PMCPMC9214523.

30. Martini L, Brameyer S, Hoyer E, Jung K, Gerland U. Dynamics of chromosomal target search by a membrane-integrated one-component receptor. PLoS Comput Biol. 2021;17(2):e1008680. Epub 20210204. doi: 10.1371/journal.pcbi.1008680. PubMed PMID: 33539417; PubMed Central PMCID: PMCPMC7888679.

31. Stracy M, Schweizer J, Sherratt DJ, Kapanidis AN, Uphoff S, Lesterlin C. Transient non-specific DNA binding dominates the target search of bacterial DNA-binding proteins. Mol Cell. 2021;81(7):1499-514 e6. Epub 20210222. doi: 10.1016/j.molcel.2021.01.039. PubMed PMID: 33621478; PubMed Central PMCID: PMCPMC8022225.

32. Miller VL, DiRita VJ, Mekalanos JJ. Identification of toxS, a regulatory gene whose product enhances toxR-mediated activation of the cholera toxin promoter. J Bacteriol. 1989;171(3):1288-93. doi: 10.1128/jb.171.3.1288-1293.1989. PubMed PMID: 2646275; PubMed Central PMCID: PMCPMC209743.

33. Dalia AB. Natural Cotransformation and Multiplex Genome Editing by Natural Transformation (MuGENT) of Vibrio cholerae. Methods Mol Biol. 2018;1839:53-64. doi: 10.1007/978-1-4939-8685-9_6. PubMed PMID: 30047054.

34. Dalia TN, Chlebek JL, Dalia AB. A modular chromosomally integrated toolkit for ectopic gene expression in Vibrio cholerae. Sci Rep. 2020;10(1):15398. doi: 10.1038/s41598-020-72387-8. PubMed PMID: 32958839; PubMed Central PMCID: PMCPMC7505983.

35. Dalia TN, Hayes CA, Stolyar S, Marx CJ, McKinlay JB, Dalia AB. Multiplex Genome Editing by Natural Transformation (MuGENT) for Synthetic Biology in Vibrio natriegens. ACS Synth Biol. 2017;6(9):1650-5. doi: 10.1021/acssynbio.7b00116. PubMed PMID: 28571309.

36. Ducret A, Quardokus EM, Brun YV. MicrobeJ, a tool for high throughput bacterial cell detection and quantitative analysis. Nat Microbiol. 2016;1(7):16077. doi: 10.1038/nmicrobiol.2016.77. PubMed PMID: 27572972; PubMed Central PMCID: PMCPMC5010025.

37. Schindelin J, Arganda-Carreras I, Frise E, Kaynig V, Longair M, Pietzsch T, et al. Fiji: an open-source platform for biological-image analysis. Nat Methods. 2012;9(7):676-82. Epub 2012/06/30. doi: 10.1038/nmeth.2019. PubMed PMID: 22743772; PubMed Central PMCID: PMCPMC3855844.

38. Bartlett TM, Bratton BP, Duvshani A, Miguel A, Sheng Y, Martin NR, et al. A Periplasmic Polymer Curves Vibrio cholerae and Promotes Pathogenesis. Cell. 2017;168(1-2):172-85 e15. Epub 2017/01/14. doi: 10.1016/j.cell.2016.12.019. PubMed PMID: 28086090; PubMed Central PMCID: PMCPMC5287421.

39. Green VE, Klancher CA, Yamamoto S, Dalia AB. The molecular mechanism for carbon catabolite repression of the chitin response in Vibrio cholerae. PLoS Genet. 2023;19(5):e1010767. Epub 2023/05/12. doi: 10.1371/journal.pgen.1010767. PubMed PMID: 37172034; PubMed Central PMCID: PMCPMC10208484.

40. Galaxy C. The Galaxy platform for accessible, reproducible, and collaborative data analyses: 2024 update. Nucleic Acids Res. 2024;52(W1):W83-W94. doi: 10.1093/nar/gkae410. PubMed PMID: 38769056; PubMed Central PMCID: PMCPMC11223835.

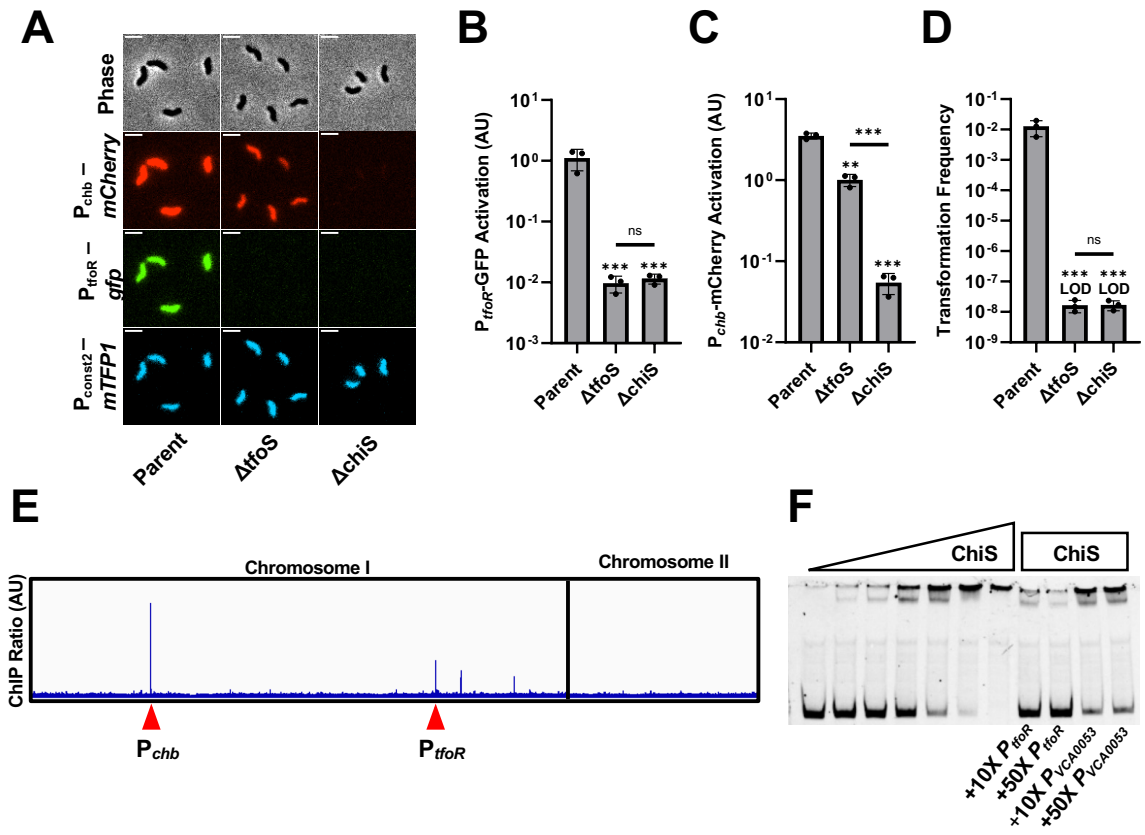

Fig. 1. *ChiS binds P_{tfoR} and is necessary for P_{tfoR} activation.* (**A-C**) Transcriptional reporter assays to assess chitin-dependent gene expression. The indicated strains all harbored 3 fluorescent reporter constructs: P_{chb}-*mCherry*, P_{tfoR}-*gfp*, and P_{const2}-*mTFP1*. Cells were incubated on chitin and then imaged via epifluorescence microscopy to assess reporter expression. Representative images are shown in **A** and the quantification of the results are shown in **B** and **C**. Scale bar, 2μm. For each replicate (n = 3), the geometric mean fluorescence was determined by analyzing 300 individual cells. (**D**) Chitin-induced natural transformation assay of the indicated strains. Results are from three independent biological replicates and shown as the mean ± SD. Statistical comparisons in **B**, **C**, and **D** were made by one-way ANOVA with Tukey's multiple comparison test on log-transformed data (normal distribution confirmed by Shapiro-Wilk test). Statistical identifiers directly above bars represent comparisons to the parent. ns, not significant. *** = $p < 0.001$, ** = $p < 0.01$. LOD, limit of detection. (**E**) ChIP-seq analysis uncovers ChiS binding sites. The panel shows the "ChIP ratio", which is defined as the mapping distribution of ChIP-enriched DNA normalized to the mapping distribution of input DNA. ChIP peaks at the P_{chb} and P_{tfoR} loci are denoted by a red arrow. (**F**) EMSAs to test ChiS binding at P_{tfoR}. Increasing concentrations of the purified ChiS cytoplasmic domain (from left to right: 0 nM, 25 nM, 50 nM, 100 nM, 200 nM, 400 nM, 800 nM) were incubated with Cy5-labeled P_{tfoR} DNA probe. Cold competitor EMSAs were carried out using 200 nM ChiS and either 10-fold or 50-fold excess of the unlabeled competitor DNA probe as indicated. Data in **F** are representative of three independent experiments.

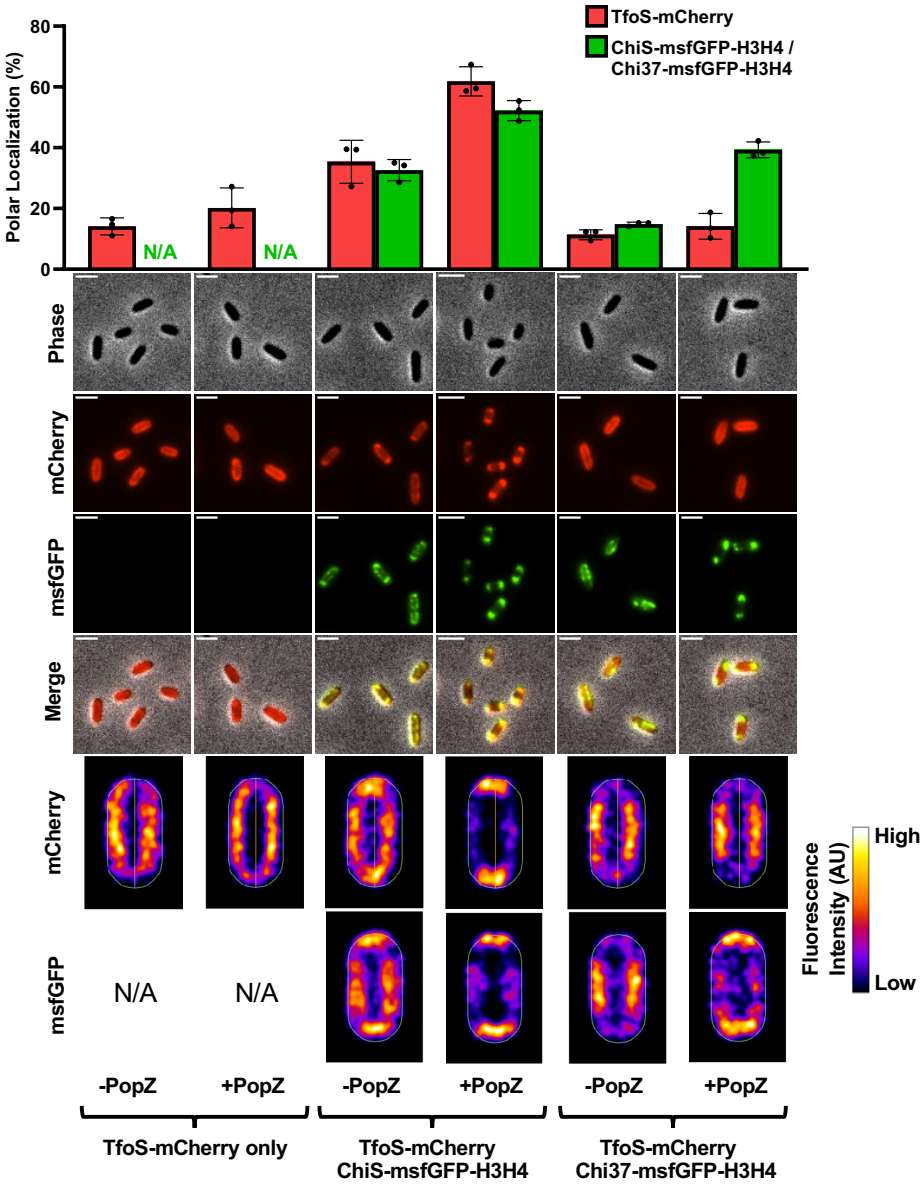

Fig. 2. *ChiS interacts with TfoS.* POLAR assays were conducted to assess the interaction between ChiS and TfoS. Colocalization was assessed in cells containing P_{bad}-*popZ* and the indicated ChiS and TfoS fusion constructs. The localization of these constructs was assessed in the absence (-PopZ) and presence (+PopZ) of PopZ induction. Scale bar, 2μm. Representative images of cells are shown along with heat maps that represent the fluorescence localization in 300 cells. Data are representative of three independent biological replicates. The proportion of TfoS-mCherry (red bars) and ChiS-msfGFP-H3H4 / Chi37-msfGFP-H3H4 (green bars) fluorescence within the polar region (≤ 0.2 μm from the cell pole) was quantified. For each replicate (n = 3), fluorescence localization was determined by analyzing 300 individual cells. N/A, not applicable

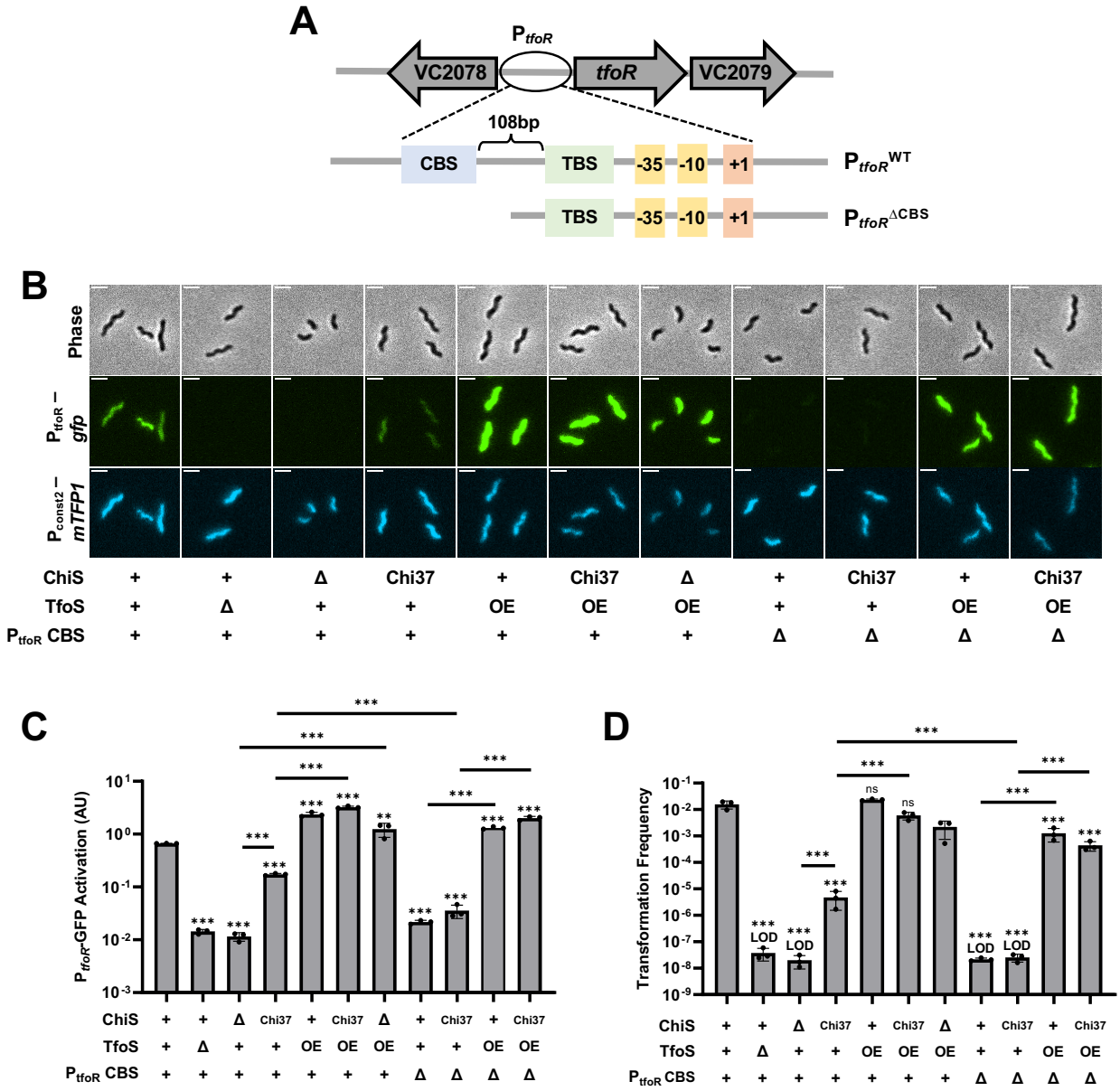

Fig. 3. *ChiS binding at P_{tfoR} is critical for activation when TfoS is expressed at native levels.* Strains harbored P_{tfoR}-*gfp,* P_{const2}-*mTFP1*, and the indicated mutations. Cells were incubated on chitin and then imaged via epifluorescence microscopy to assess reporter expression. For ChiS genotypes, "+" denotes that cells have a WT copy of ChiS, "Δ" denotes that cells lack ChiS, and "Chi37" indicates that cells express the Chi37 chimera instead of ChiS. For TfoS, "+" denotes $TfoS^{WT}$, "Δ" denotes that TfoS is deleted, and "OE" denotes that TfoS is overexpressed (P_{tac}-*tfoS* + 1μM IPTG). For P_{tfoR} CBS, "+" denotes the full-length wildtype P_{tfoR} promoter while "Δ" denotes $P_{tfoR}^{\Delta CBS}$. (**A**) Schematic of the P_{tfoR} and $P_{tfoR}^{\Delta CBS}$ reporters, highlighting the organization of the ChiS Binding Site (CBS), the TfoS Binding Site (TBS), the -35 and -10 elements, and the transcriptional start site (+1). (**B**) Representative images of cells. Scale bar, 2μm. (**C**) Quantification of P_{tfoR}-*gfp* reporter activity. For each replicate (*n* = 3), the geometric mean fluorescence was determined by analyzing 300 individual cells. (**D**) Chitin-dependent transformation assays of the indicated strains. The mutations in P_{tfoR} were present in both the

856 P_{tfoR}-*gfp* reporter construct and the native P_{tfoR} locus for transcriptional reporter assays, and at
857 the native P_{tfoR} locus for transformation assays. Results are from three independent biological
858 replicates and shown as the mean ± SD. Statistical comparisons in **C** and **D** are made by one-
859 way ANOVA with Tukey's multiple comparison test on the log-transformed data (normal
860 distribution confirmed by Shapiro-Wilk test for all samples except "Δ*chiS* TfoS OE" in **D**, which
861 was excluded from the analysis). Statistical identifiers directly above bars represent
862 comparisons to the parent. ns, not significant. *** = $p < 0.001$, ** = $p < 0.01$. LOD, limit of
863 detection.
864

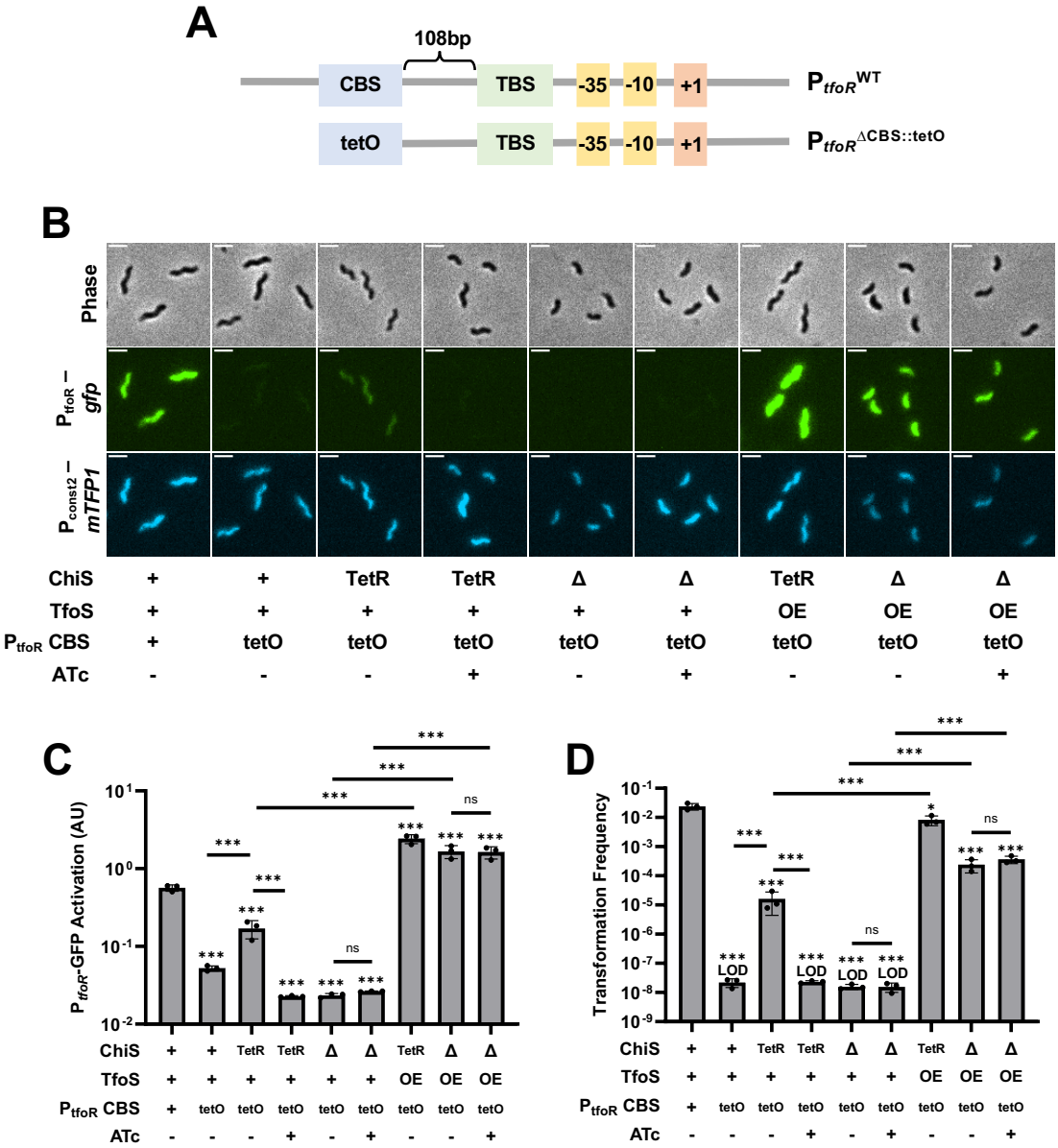

Fig. 4. *Recruitment of P_{tfoR} to the membrane is sufficient for TfoS-dependent activation.* Strains harbored P_{tfoR}-*gfp,* P_{const2}-*mTFP1*, and the indicated mutations. Cells were incubated on chitin and then imaged via epifluorescence microscopy to assess reporter expression. For ChiS genotypes, "+" denotes that cells have a WT copy of ChiS, "Δ" denotes that cells lack ChiS, and "TetR" indicates that cells express a $ChiS^{\Delta DBD}$-TetR fusion. For TfoS, "+" denotes $TfoS^{WT}$, "Δ" denotes that TfoS is deleted, and "OE" denotes that TfoS is overexpressed (P_{tac}-*tfoS* + 1μM IPTG). For P_{tfoR} CBS, "+" denotes the full-length wildtype P_{tfoR} promoter while "tetO" denotes $P_{tfoR}^{\Delta CBS::tetO}$. Where indicated, 50 ng/mL ATc was added to the reaction. (**A**) Schematic of the P_{tfoR} and $P_{tfoR}^{\Delta CBS::tetO}$ reporters, highlighting the organization of the ChiS Binding Site (CBS), the TfoS Binding Site (TBS), the Tet operator (tetO) site, the -35 and -10 elements, and the transcriptional start site (+1). (**B**) Representative images of cells. Scale bar, 2μm. (**C**) Quantification of P_{tfoR}-*gfp* reporter activity. For each replicate (n = 3), the geometric mean fluorescence was determined by analyzing 300 individual cells. (**D**) Chitin-dependent transformation assays of the indicated strains. The mutations in P_{tfoR} were present in the P_{tfoR}-

881 *gfp* reporter construct for transcriptional reporter assays, but at the native locus for
882 transformation assays. Results are from three independent biological replicates and shown as
883 the mean ± SD. Statistical comparisons in **C** and **D** are made by one-way ANOVA with Tukey's
884 multiple comparison test on the log-transformed data (normal distribution confirmed by Shapiro-
885 Wilk test). Statistical identifiers directly above bars represent comparisons to the parent. ns, not
886 significant. *** = $p < 0.001$, ** = $p < 0.01$. LOD, limit of detection.
887

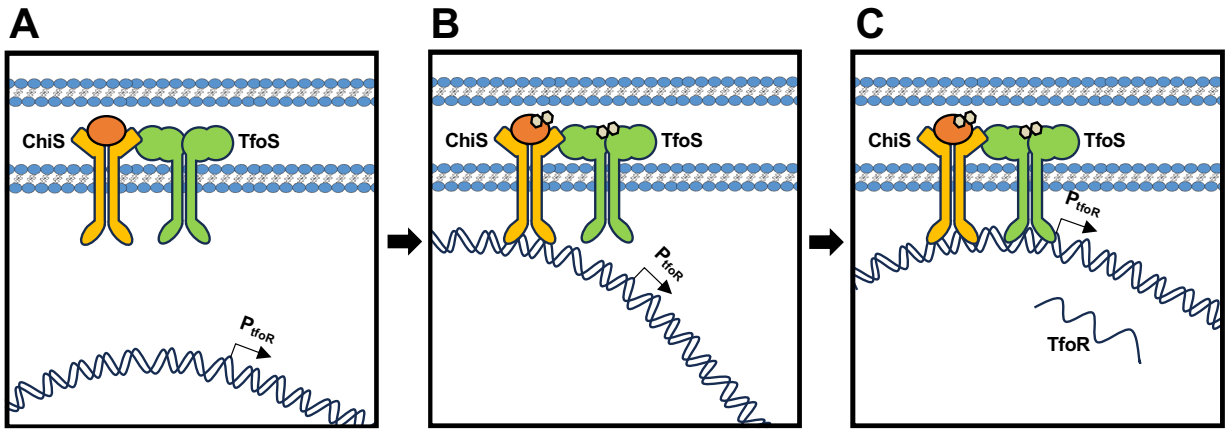

Fig. 5. *Proposed model for chitin-induced activation of P_{tfoR}.* (**A**) In the absence of chitin oligosaccharides (tan hexagons), ChiS and TfoS are inactive. In the presence of chitin, (**B**) ChiS and TfoS are activated and ChiS binds upstream of the *tfoR* promoter. ChiS binds to TfoS, thereby recruiting it to the membrane-localized P_{tfoR}. (**C**) These combined activities of ChiS allow TfoS to subsequently bind P_{tfoR} and activate transcription of the *tfoR* small RNA that is critical for chitin-induced natural transformation.

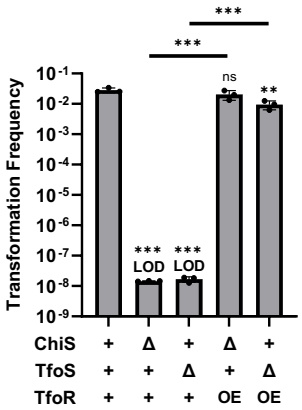

Fig. S1. *Overexpression of tfoR recovers transformation in ΔchiS and ΔtfoS backgrounds.* Chitin-dependent transformation assays of the indicated strains. For ChiS genotypes, "+" denotes that cells have a WT copy of ChiS and "Δ" denotes that cells lack ChiS. For TfoS genotypes, "+" denotes $TfoS^{WT}$ and "Δ" denotes that TfoS is deleted. For *tfoR*, "+" denotes WT *tfoR* and "OE" denotes that *tfoR* is overexpressed (P_{tac}-*tfoR* + 1μM IPTG). Results are from three independent biological replicates and shown as mean ± SD. Statistical comparisons are made by one-way ANOVA with Tukey's multiple comparison test on the log-transformed data (normal distribution confirmed by Shapiro-Wilk test). Statistical identifiers directly above bars represent comparisons to the parent. ns, not significant. *** = $p < 0.001$, ** = $p < 0.01$. LOD, limit of detection.

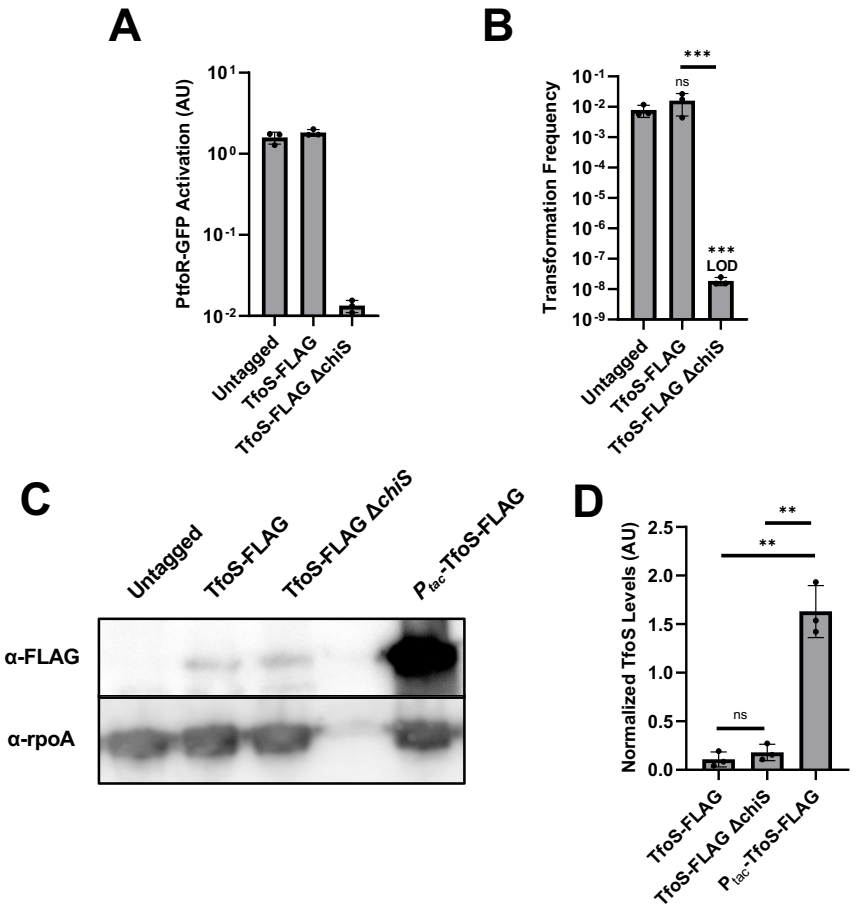

Fig. S2. *ChiS does not alter TfoS expression.* (**A**) Transcriptional reporter assays to assess chitin-dependent gene expression in the indicated strains. All strains harbored P_{tfoR}-*gfp* and P_{const2}-*mTFP1* constructs. Cells were incubated on chitin and then imaged via epifluorescence microscopy to assess reporter expression. For each replicate (n = 3), the geometric mean fluorescence was determined by analyzing 300 individual cells. (**B**) Chitin-dependent transformation assays of indicated strains. (**C**) Western blot analysis of the indicated strains. The blot in **C** is representative of three biological replicates. (**D**) Quantification of TfoS levels from western blots. For each replicate (n = 3), the normalized TfoS level was determined by dividing the intensity of the TfoS band by the intensity of the RpoA band. Results in **A**, **B**, and **D** are from three independent biological replicates and shown as the mean ± SD. Statistical comparisons in **B** and **D** were made by one-way ANOVA with Tukey's multiple comparison test (normal distribution confirmed by Shapiro-Wilk test). Statistical identifiers directly above bars represent comparisons to the parent. ns, not significant. *** = $p < 0.001$, ** = $p < 0.01$. LOD, limit of detection.

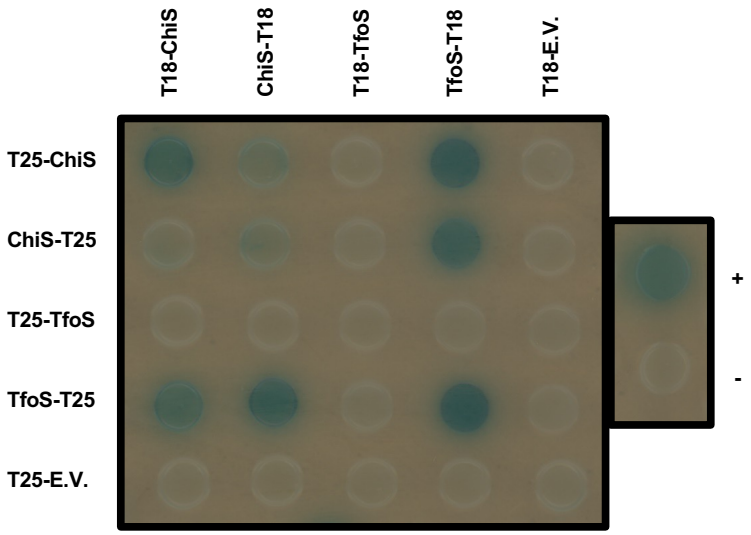

Fig. S3. *ChiS interacts with TfoS*. BACTH assess interactions between ChiS and TfoS. For BACTH assays, ChiS and TfoS either had an N-terminal fusion (indicated as TXX-protein) or a C-terminal fusion (indicated as protein-TXX) to the T25 or T18 fragment of adenylate cyclase.“+” and “-” indicate positive (T18-zip + T25-zip) and negative (T18 E.V. + T25 E.V.) controls for the assay. “E.V.” denotes an empty vector.

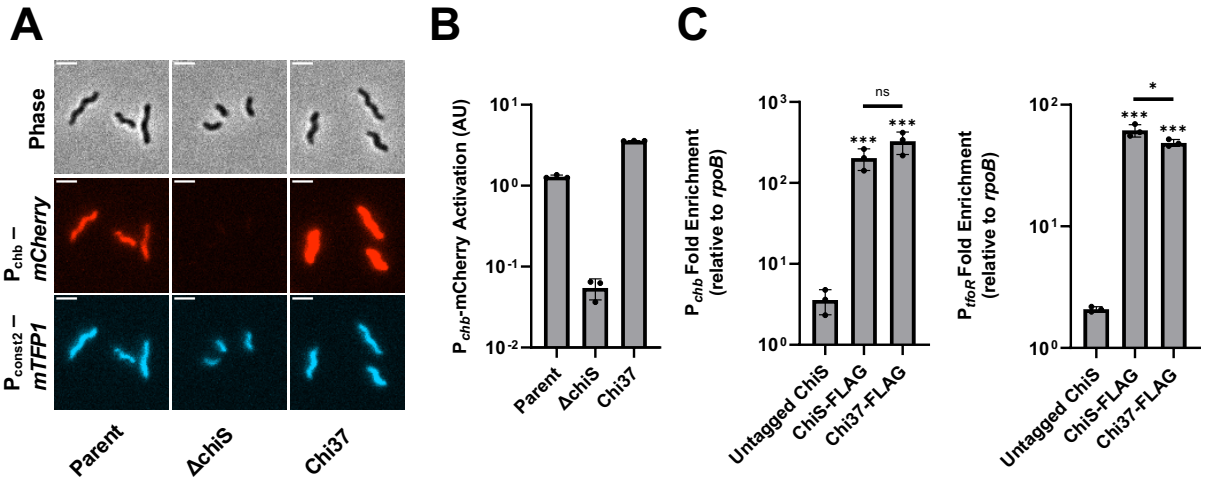

935
936
937 **Fig. S4**. *Chi37 is a functional chimera of ChiS*. (**A**-**B**) Transcriptional reporter assays to assess
938 chitin-dependent gene expression in the indicated strains. All strains harbored P_{chb}-*mCherry* and
939 P_{const2}-*mTFP1* constructs. Cells were incubated on chitin and then imaged via epifluorescence
940 microscopy to assess reporter expression. Representative images are shown in **A** and the
941 quantification of the results are shown in **B**. For each replicate (n = 3), the geometric mean
942 fluorescence was determined by analyzing 300 individual cells. (**C**) ChIP-qPCR assays were
943 performed with the indicated strains to assess ChiS and Chi37 binding at P_{chb} and P_{tfoR} *in vivo*.
944 Results are from three independent biological replicates and shown as the mean ± SD.
945 Statistical comparisons were made by one-way ANOVA with Tukey's multiple comparison test
946 (normal distribution confirmed by Shapiro-Wilk test). Statistical identifiers directly above bars
947 represent comparisons to the parent. ns, not significant. *** = $p < 0.001$, * = $p < 0.05$.
948

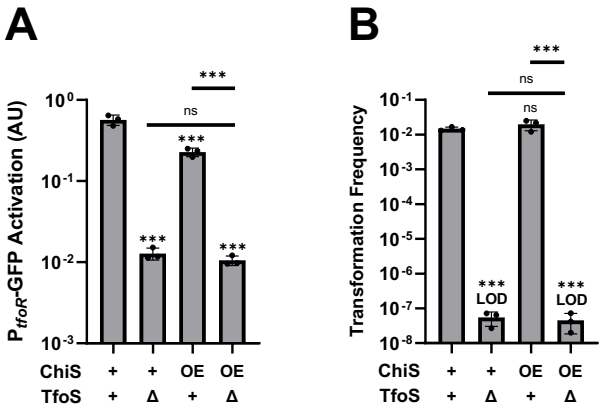

Fig. S5. *Overexpression of ChiS does not restore P_{tfoR} activation in the absence of TfoS.* (**A**) Transcriptional reporter assays to assess chitin-dependent gene expression in the indicated strains. For ChiS genotypes, "+" denotes cells that have a WT copy of ChiS, and "OE" denotes that ChiS is overexpressed (P_{tac}-*chiS* + 1μM IPTG). For TfoS genotypes, "+" indicates that cells have a WT copy of TfoS, while "Δ" denotes that cells lack TfoS. All strains harbored P_{tfoR}-*gfp* and P_{const2}-*mTFP1* constructs. For each replicate (n = 3), the geometric mean was determined by analyzing 300 individual cells. (**B**) Chitin-dependent transformation assays of the indicated strains. Results are from three independent biological replicates and shown as mean ± SD. Statistical comparisons were made by one-way ANOVA with Tukey's multiple comparison test on the log-transformed data (normal distribution confirmed by Shapiro-Wilk test). Statistical identifiers directly above bars represent comparisons made to the parent. *** = $p < 0.001$, ns = not significant. LOD, limit of detection.

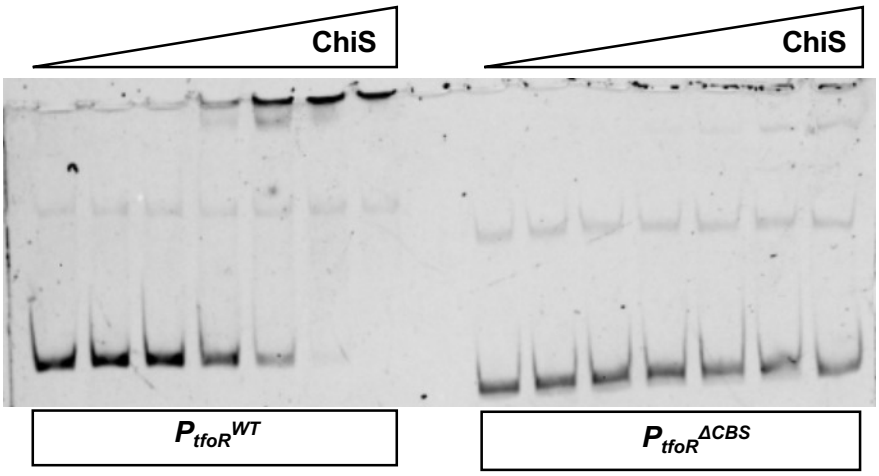

964
965
966 **Fig. S6**. *Truncating the 5' end of P_{tfoR} removes the ChiS binding site.* EMSAs of the purified
967 ChiS cytoplasmic domain with the indicated probe DNA. Increasing concentrations of ChiS
968 (from left to right: 0 nM, 25 nM, 50 nM, 100 nM, 200 nM, 400 nM, 800 nM) were incubated with
969 the indicated Cy5-labelled P_{tfoR} DNA probe. P_{tfoR}^{WT} denotes the full-length wildtype P_{tfoR}
970 promoter, while $P_{tfoR}^{\Delta CBS}$ denotes the truncated promoter where the ChiS binding site was
971 removed from P_{tfoR}. Data are representative of three independent experiments.
972

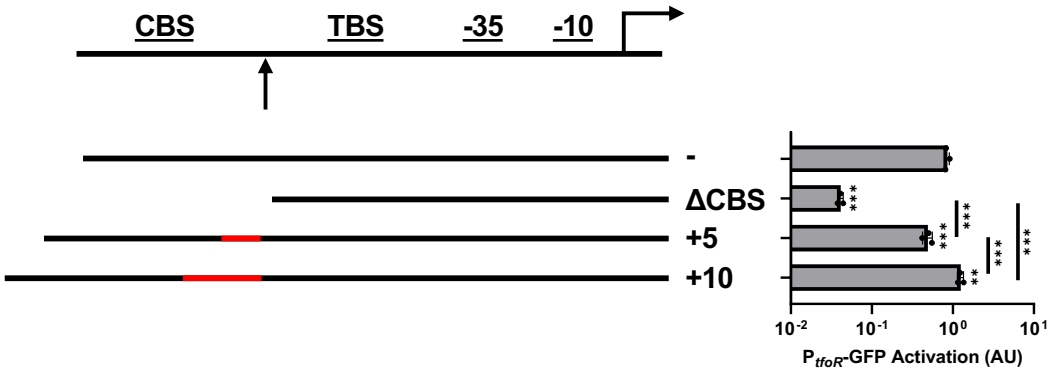

973
974
975 **Fig. S7**. *Phasing between the ChiS and TfoS binding sites is not critical for P_{tfoR} activation.*
976 Transcriptional reporter assays to assess chitin-dependent gene expression of strains with the
977 indicated P_{tfoR}-*gfp* reporter constructs. Schematic of the P_{tfoR} reporter constructs depicts where
978 insertions of 5 bp or 10 bp (red) were introduced in between the ChiS binding site (CBS) and
979 TfoS binding site (TBS) (see arrow) to alter the phasing between these elements. Activation of
980 these reporters can be be compared to the parent P_{tfoR} reporter (positive control) and the
981 $P_{tfoR}^{\Delta CBS}$ (negative control). Data are from three biological replicates (300 cells analyzed per
982 replicate) and shown as the geometric mean ± SD. Statistical comparisons were made by one-
983 way ANOVA with Tukey's multiple comparison test on the log-transformed data (normal
984 distribution confirmed by Shapiro-Wilk test). Statistical identifiers directly above bars represent
985 comparisons made to the parent (top bar). ** = $p < 0.01$, *** = $p < 0.001$.
986

987 **Table S1.** *Strains used in this study.*
988

Strain ID	Genotype	Reference in Manuscript
SAD030	*V. cholerae* WT E7946 Sm^R	Parent for all *V. cholerae* strains in this study Fig. S1 ChiS+ TfoS+ TfoR+
SAD3634 / ACH0004	igVCA0265-66::$Spec^R$-P_{const2}-*mTFP1*; ΔVCA0692::Tm^R-P_{tfoR}-*gfp*; Δ*lacZ*::Kan^R-P_{chb}-*mCherry*	Fig. 1A-D Parent
SAD3635 / ACH0014	igVCA0265-66::$Spec^R$-P_{const2}-*mTFP1*; ΔVCA0692::Tm^R-P_{tfoR}-*gfp*; Δ*lacZ*::Kan^R-P_{chb}-*mCherry*; Δ*tfoS*::Zeo^R	Fig. 1A-D ΔtfoS
SAD3636 / ACH0019	igVCA0265-66::$Spec^R$-P_{const2}-*mTFP1*; ΔVCA0692::Tm^R-P_{tfoR}-*gfp*; Δ*lacZ*::Kan^R-P_{chb}-*mCherry*; Δ*chiS*::$Carb^R$	Fig. 1A-D, Fig. 3B-D, Fig. S4A-B ΔchiS / ΔchiS TfoS+ P_{tfoR} CBS+
SAD3653 / ACH0205	Δ*crvA*::Zeo^R; igVCA0265-66::Cm^R-P_{bad}-*popZ*; Δ*lacZ*::$Spec^R$-P_{tac}-*tfoS*-L5-*mCherry*	Fig. 2 TfoS-mCherry only
SAD3652 / ACH0204	Δ*crvA*::Zeo^R; igVCA0265-66::Cm^R-P_{bad}-*popZ*; Δ*lacZ*::$Spec^R$-P_{tac}-*tfoS*-L5-*mCherry*; ΔVCA0692::Tm^R-P_{tac}-*chiS-msfGFP*-H3H4	Fig. 2 TfoS-mCherry ChiS-msfGFP-H3H4
SAD3654 / ACH0207	Δ*crvA*::Zeo^R; igVCA0265-66::Cm^R-P_{bad}-*popZ*; Δ*lacZ*::$Spec^R$-P_{tac}-*tfoS*-L5-*mCherry*; ΔVCA0692::Tm^R-P_{tac}-*chi37-msfGFP*-H3H4	Fig. 2 TfoS-mCherry Chi37-msfGFP-H3H4
SAD3645 / ACH0142	igVCA0265-66::$Spec^R$-P_{const2}-*mTFP1*; ΔVCA0692::Tm^R-P_{tfoR}-*gfp*; Δ*lacZ*::Kan^R-P_{chb}-*mCherry*; Δ*chiS*::$Carb^R$; igVCA0587-88::Erm^R-P_{chiS}-*chiS*	Fig. 3B-D ; Fig. 4B-D ; Fig. S4A-B ; Fig. S5 ChiS+ TfoS+ P_{tfoR} CBS+
SAD3655 / ACH0273	igVCA0265-66::$Spec^R$-P_{const2}-*mTFP1*; ΔVCA0692::Tm^R-P_{tfoR}-*gfp*; Δ*lacZ*::Kan^R-P_{chb}-*mCherry*; Δ*chiS*::$Carb^R$; igVCA0587-88::Erm^R-P_{chiS}-*chiS*; Δ*tfoS*::Zeo^R	Fig. 3B-D ; Fig. S5 ChiS+ ΔtfoS P_{tfoR} CBS+
SAD3644 / ACH0141	igVCA0265-66::$Spec^R$-P_{const2}-*mTFP1*; ΔVCA0692::Tm^R-P_{tfoR}-*gfp*; Δ*lacZ*::Kan^R-P_{chb}-*mCherry*; Δ*chiS*::$Carb^R$; igVCA0587-88::Erm^R-P_{chiS}-*chi37*	Fig. 3B-D ; Fig. S4A-B Chi37 TfoS+ P_{tfoR} CBS+
SAD3647 / ACH0144	igVCA0265-66::$Spec^R$-P_{const2}-*mTFP1*; ΔVCA0692::Tm^R-P_{tfoR}-*gfp*; Δ*chiS*::$Carb^R$; igVCA0587-88::Erm^R-P_{chiS}-*chiS*; Δ*lacZ*::Zeo^R-P_{tac}-*tfoS*	Fig. 3B-D ChiS+ TfoS OE P_{tfoR} CBS+
SAD3646 / ACH0143	igVCA0265-66::$Spec^R$-P_{const2}-*mTFP1*; ΔVCA0692::Tm^R-P_{tfoR}-*gfp*; Δ*chiS*::$Carb^R$; igVCA0587-88::Erm^R-P_{chiS}-*chi37*; Δ*lacZ*::Zeo^R-P_{tac}-*tfoS*	Fig. 3B-D Chi37 TfoS OE P_{tfoR} CBS+
SAD3648 / ACH0147	igVCA0265-66::$Spec^R$-P_{const2}-*mTFP1*; ΔVCA0692::Tm^R-P_{tfoR}-*gfp*; Δ*chiS*::$Carb^R$; Δ*lacZ*::Zeo^R-P_{tac}-*tfoS*	Fig. 3B-D ΔchiS TfoS OE P_{tfoR} CBS+
SAD3678 / ACH0499	igVCA0265-66::$Spec^R$-P_{const2}-*mTFP1*; ΔVCA0692::Tm^R-$P_{tfoR}^{\Delta CBS}$-*gfp*; $P_{tfoR}^{\Delta CBS}$; Δ*chiS*::$Carb^R$; igVCA0587-88::Erm^R-P_{chiS}-*chiS*	Fig. 3B-C ChiS+ TfoS+ ΔP_{tfoR} CBS

SAD3679 / ACH0500	igVCA0265-66::Spec^R-P$_{const2}$-*mTFP1*; ΔVCA0692::Tm^R-P$_{tfoR}$ $^{\Delta CBS}$-*gfp*; P$_{tfoR}$$^{\Delta CBS}$; Δ*chiS*::Carb^R; igVCA0587-88::Erm^R-P$_{chiS}$-*chiS*; Δ*lacZ*::Zeo^R-P$_{tac}$-*tfoS*	Fig. 3B-C ChiS+ TfoS OE ΔP$_{tfoR}$ CBS
SAD3681 / ACH0504	igVCA0265-66::Spec^R-P$_{const2}$-*mTFP1*; ΔVCA0692::Tm^R-P$_{tfoR}$ $^{\Delta CBS}$-*gfp*; P$_{tfoR}$$^{\Delta CBS}$; Δ*chiS*::Carb^R; igVCA0587-88::Erm^R-P$_{chiS}$-*chi37*	Fig. 3B-C Chi37 TfoS+ ΔP$_{tfoR}$ CBS
SAD3680 / ACH0502	igVCA0265-66::Spec^R-P$_{const2}$-*mTFP1*; ΔVCA0692::Tm^R-P$_{tfoR}$ $^{\Delta CBS}$-*gfp*; P$_{tfoR}$$^{\Delta CBS}$; Δ*chiS*::Carb^R; igVCA0587-88::Erm^R-P$_{chiS}$-*chi37*; Δ*lacZ*::Zeo^R-P$_{tac}$-*tfoS*	Fig. 3B-C Chi37 TfoS OE ΔP$_{tfoR}$ CBS
SAD3656 / ACH0278	igVCA0265-66::Spec^R-P$_{const2}$-*mTFP1*; ΔVCA0692::Tm^R-P$_{tfoR}$-*gfp*; Δ*lacZ*::Kan^R-P$_{chb}$-*mCherry*; Δ*chiS*::Carb^R; igVCA0587-88::Erm^R-P$_{chiS}$-*chi37*; P$_{tfoR}$$^{\Delta CBS}$; ΔVC1807::Smx^R	Fig. 3D Chi37 TfoS+ ΔP$_{tfoR}$ CBS
SAD3657 / ACH0279	igVCA0265-66::SpecR-P$_{const2}$-*mTFP1*; ΔVCA0692::TmR-P$_{tfoR}$-*gfp*; ΔlacZ::KanR-P$_{chb}$-*mCherry*; Δ*chiS*::CarbR; igVCA0587-88::ErmR-P$_{chiS}$-*chiS*; P$_{tfoR}$$^{\Delta CBS}$; ΔVC1807::SmxR	Fig. 3D ChiS+ TfoS+ ΔP$_{tfoR}$ CBS
SAD3658 / ACH0280	igVCA0265-66::Spec^R-P$_{const2}$-*mTFP1*; ΔVCA0692::Tm^R-P$_{tfoR}$-*gfp*; Δ*chiS*::Carb^R; igVCA0587-88::Erm^R-P$_{chiS}$-*chi37*; P$_{tfoR}$$^{\Delta CBS}$; ΔVC1807::Smx^R; Δ*lacZ*::Zeo^R-P$_{tac}$-*tfoS*	Fig. 3D Chi37 TfoS OE ΔP$_{tfoR}$ CBS
SAD3659 / ACH0281	igVCA0265-66::Spec^R-P$_{const2}$-*mTFP1*; ΔVCA0692::Tm^R-P$_{tfoR}$-*gfp*; Δ*chiS*::Carb^R; igVCA0587-88::Erm^R-P$_{chiS}$-*chiS*; P$_{tfoR}$$^{\Delta CBS}$; ΔVC1807::Smx^R; Δ*lacZ*::Zeo^R-P$_{tac}$-*tfoS*	Fig. 3D ChiS+ TfoS OE ΔP$_{tfoR}$ CBS
SAD3670 / ACH0374	igVCA0265-66::Spec^R-P$_{const2}$-*mTFP1*; ΔVCA0692::Tm^R-P$_{tfoR}$$^{\Delta CBS::tetO}$-*gfp*; Δ*lacZ*::Kan^R-P$_{chb}$-*mCherry*; Δ*chiS*::Carb^R; igVCA0587-88::Erm^R-P$_{chiS}$-*chiS*	Fig. 4B-C ChiS+ TfoS+ P$_{tfoR}$ CBS tetO
SAD3666 / ACH0310	igVCA0265-66::Spec^R-P$_{const2}$-*mTFP1*; ΔVCA0692::Tm^R-P$_{tfoR}$$^{\Delta CBS::tetO}$-*gfp*; Δ*lacZ*::Kan^R-P$_{chb}$-*mCherry*; Δ*chiS*::Carb^R; igVCA0587-88::Erm^R-P$_{chiS}$-*chiS*$^{\Delta DBD}$-*TetR*	Fig. 4B-C ChiS TetR TfoS+ P$_{tfoR}$ CBS tetO
SAD3667 / ACH0325	igVCA0265-66::Spec^R-P$_{const2}$-*mTFP1*; ΔVCA0692::Tm^R-P$_{tfoR}$$^{\Delta CBS::tetO}$-*gfp*; Δ*lacZ*::Kan^R-P$_{chb}$-*mCherry*; Δ*chiS*::Carb^R	Fig. 4B-C ΔchiS TfoS+ P$_{tfoR}$ CBS tetO
SAD3668 / ACH0338	igVCA0265-66::Spec^R-P$_{const2}$-*mTFP1*; ΔVCA0692::Tm^R-P$_{tfoR}$$^{\Delta CBS::tetO}$-*gfp*; Δ*chiS*::Carb^R; igVCA0587-88::Erm^R-P$_{chiS}$-*chiS*$^{\Delta DBD}$-*TetR*; Δ*lacZ*::Zeo^R-P$_{tac}$-*tfoS*	Fig. 4B-C ChiS TetR TfoS OE P$_{tfoR}$ CBS tetO
SAD3669 / ACH0340	igVCA0265-66::Spec^R-P$_{const2}$-*mTFP1*; ΔVCA0692::Tm^R-P$_{tfoR}$$^{\Delta CBS::tetO}$-*gfp*; Δ*lacZ*::Kan^R-P$_{chb}$-*mCherry*; Δ*chiS*::Carb^R; Δ*lacZ*::Zeo^R-P$_{tac}$-*tfoS*	Fig. 4B-C ΔchiS TfoS OE P$_{tfoR}$ CBS tetO
SAD3674 / ACH0401	Δ*chiS*::Carb^R; igVCA0587-88::Erm^R-P$_{chiS}$-*chiS*; P$_{tfoR}$$^{\Delta CBS::tetO}$; ΔVC1807::Smx^R	Fig. 4D ChiS+ TfoS+ P$_{tfoR}$ CBS tetO

SAD3672 / ACH0399	Δ*chiS*::Carb^R; igVCA0587-88::Erm^R-P$_{chiS}$-*chiS*$^{\Delta DBD}$-*TetR*; P$_{tfoR}^{\Delta CBS::tetO}$; ΔVC1807::Smx^R	Fig. 4D ChiS TetR TfoS+ P$_{tfoR}$ CBS tetO
SAD3671 / ACH0398	Δ*chiS*::Carb^R; P$_{tfoR}^{\Delta CBS::tetO}$; ΔVC1807::Smx^R	Fig. 4D ΔchiS TfoS+ P$_{tfoR}$ CBS tetO
SAD3673 / ACH0400	Δ*chiS*::Carb^R; igVCA0587-88::Erm^R-P$_{chiS}$-*chiS*$^{\Delta DBD}$-*TetR*; P$_{tfoR}^{\Delta CBS::tetO}$; ΔVC1807::Smx^R; Δ*lacZ*::Zeo^R-P$_{tac}$-*tfoS*	Fig. 4D ChiS TetR TfoS OE P$_{tfoR}$ CBS tetO
SAD3677 / ACH0418	Δ*chiS*::Carb^R; P$_{tfoR}^{\Delta CBS::tetO}$; ΔVC1807::Smx^R; Δ*lacZ*::Zeo^R-P$_{tac}$-*tfoS*	Fig. 4D ΔchiS TfoS OE P$_{tfoR}$ CBS tetO
SAD3662 / ACH0288	Δ*chiS*::Carb^R	Fig. S1 ΔchiS TfoS+ TfoR+
SAD3663 / ACH0289	Δ*tfoS*::Zeo^R	Fig. S1 ChiS+ ΔtfoS TfoR+
SAD3664 / ACH0290	Δ*chiS*::Carb^R; Δ*lacZ*::Spec^R-P$_{tac}$-*tfoR*	Fig. S1 ΔchiS TfoS+ TfoR OE
SAD3665 / ACH0291	Δ*tfoS*::Zeo^R; Δ*lacZ*::Spec^R-P$_{tac}$-*tfoR*	Fig. S1 ChiS+ ΔtfoS TfoR OE
SAD3650 / ACH0186	igVCA0265-66::Spec^R-P$_{const2}$-*mTFP1*; Δ*lacZ*::Kan^R-P$_{tfoR}$-*gfp*; ΔVC1807::Cm^R	Fig. S2 Untagged
SAD3649 / ACH0185	igVCA0265-66::Spec^R-P$_{const2}$-*mTFP1*; Δ*lacZ*::Kan^R-P$_{tfoR}$-*gfp*; ΔVC1807::Cm^R; *tfoS* N929 1X FLAG	Fig. S2 TfoS-FLAG
SAD3651 / ACH0189	igVCA0265-66::Spec^R-P$_{const2}$-*mTFP1*; Δ*lacZ*::Kan^R-P$_{tfoR}$-*gfp*; ΔVC1807::Cm^R; *tfoS* N929 1X FLAG; Δ*chiS*::Carb^R	Fig. S2 TfoS-FLAG ΔchiS
SAD3661 / ACH0286	igVCA0265-66::Spec^R-P$_{const2}$-*mTFP1*; ΔVC1807::Cm^R; Δ*lacZ*::Zeo^R-P$_{tac}$-*tfoS N929 1X FLAG*	Fig. S2 Ptac-TfoS-FLAG
SAD3637 / ACH0031	TG1, pKT25-ChiS Kan^R	Fig. S3 T25-ChiS
SAD3640 / ACH0035	TG1, pKT25-TfoS Kan^R	Fig. S3 T25-TfoS
SAD3683 / VEG0253	TG1, pKNT25-ChiS Kan^R	Fig. S3 ChiS-T25
SAD3641 / ACH0036	TG1, pKNT25-TfoS Kan^R	Fig. S3 TfoS-T25
SAD3638 / ACH0033	TG1, pUT18C-ChiS Carb^R	Fig. S3 T18-ChiS
SAD3642 / ACH0037	TG1, pUT18C-TfoS Carb^R	Fig. S3 T18-TfoS

SAD3639 / ACH0034	TG1, pUT18-ChiS Carb^R	Fig. S3 ChiS-T18
SAD3643 / ACH0038	TG1, pUT18-TfoS Carb^R	Fig. S3 TfoS-T18
SAD2236	TG1, pKT25 vector Kan^R	Fig. S3 T25-E.V.
SAD2240	TG1, pUT18C vector Carb^R	Fig. S3 T18-E.V.
SAD2238	TG1, pKT25-zip Kan^R	Fig. S3 T25-zip
SAD2241	TG1, pUT18C-*zip* Carb^R	Fig. S3 T18-zip
SAD3354 / VEG0565	Δ*lacZ*::Kan^R-P$_{chb}$-*gfp*; Δ*chiS/cbp*::Carb^R; ΔVCA0692::*Tm^R*-P$_{chiS}$-*chiS*	Fig. S4C Untagged ChiS
SAD2706 / TND1801	Δ*lacZ*::Kan^R-P$_{chb}$-*gfp*; Δ*chiS/cbp*::Carb^R; ΔVCA0692::Tm^R-P$_{chiS}$-*chiS* 1X FLAG after E566	Fig. S4C ChiS-FLAG
SAD3682 / CAK672	Δ*lacZ*::Kan^R-P$_{chb}$-*gfp*; Δ*chiS/cbp*::Carb^R; ΔVCA0692::Tm^R-P$_{chiS}$-*chi37* 3X FLAG	Fig. S4C Chi37-FLAG
SAD3675 / ACH0411	igVCA0265-66::Spec^R-P$_{const2}$-*mTFP1*; ΔVCA0692::Tm^R-P$_{tfoR}$-*gfp*; Δ*lacZ*::Kan^R-P$_{chb}$-*mCherry*; Δ*chiS*::Carb^R; igVCA0587-88::Erm^R-P$_{tac}$-*chiS E566 1X FLAG*	Fig. S5 ChiS OE TfoS+
SAD3676 / ACH0414	igVCA0265-66::Spec^R-P$_{const2}$-*mTFP1*; ΔVCA0692::Tm^R-P$_{tfoR}$-*gfp*; Δ*lacZ*::Kan^R-P$_{chb}$-*mCherry*; Δ*chiS*::Carb^R; igVCA0587-88::Erm^R-P$_{tac}$-*chiS E566 1X FLAG*; Δ*tfoS*::Zeo^R	Fig. S5 ChiS OE ΔtfoS
SAD3684 / TND4270	igVCA0265-66::Spec^R-P$_{const2}$-*mTFP1*; ΔVCA0692::Tm^R-P$_{tfoR}$-*gfp*	Fig. S7 -
SAD3685 / TND4271	igVCA0265-66::Spec^R-P$_{const2}$-*mTFP1*; ΔVCA0692::Tm^R-P$_{tfoR}^{+5bp}$-*gfp*	Fig. S7 +5
SAD3686 / TND4272	igVCA0265-66::Spec^R-P$_{const2}$-*mTFP1*; ΔVCA0692::Tm^R-P$_{tfoR}^{+10bp}$-*gfp*	Fig. S7 +10
SAD3660 / ACH0284	igVCA0265-66::Spec^R-P$_{const2}$-*mTFP1*; ΔVCA0692::Tm^R-P$_{tfoR}^{\Delta CBS}$-*gfp*; Δ*chiS*::Carb^R; igVCA0587-88::Erm^R-P$_{chiS}$-*chiS*	Fig. S7 ΔCBS

**Double identifiers under "Strain ID" refer to the same strain that has been stocked in two independent strain collections.*

992 **Table S2.** *Primers used in this study.*
993

Primers for SOE Deletions		
Primer	**Sequence**	**Description**
ABD123	ATTCCGGGGATCCGTCGAC	Antibiotic resistance cassette F
ABD124	TGTAGGCTGGAGCTGCTTC	Antibiotic resistance cassette R
ABD767	TTAATTTGGATCCCTGCGACACTC	ΔchiS F1 for Up arm
ABD768	gtcgacggatccccggaatCAAAAAACGTGAGGAGA ATGCC	ΔchiS R1 for Up arm
ABD769	gaagcagctccagcctacaTTCTTGAGCATTGCAAAG AAGC	ΔchiS F2 for Down arm
ABD770	CTGGAACGAATGAAGAAGTCCAG	ΔchiS R2 for Down arm
ABD640	GCAATACACGCTGTGTTTCACCG	ΔtfoS F1 for Up arm
ABD641	gtcgacggatccccggaatCAATTCAAGAATTCGTGCTTTATTGG	ΔtfoS R1 for Up arm
ABD642	gaagcagctccagcctacaTAATAGAGCCCATCTCTATTTCATC	ΔtfoS F2 for Down arm
ABD643	TCGTTTTCTAAGGCTCGAATCGCC	ΔtfoS R2 for Down arm
BBC1782	CAAGCGATGTACGAACGAAC	ΔcrvA F1 for Up arm
BBC1783	gtcgacggatccccggaatCCACATAAAGTGGGAAAGACAAAC	ΔcrvA R1 for Up arm
BBC1784	gaagcagctccagcctacaGTCAATGGCAATGACACGG	ΔcrvA F2 for Down arm
BBC1785	GCTTGACGTTGTTGCTTACTGG	ΔcrvA R2 for Down arm
BBC717	AAATAGATTTGGTGACTTTACCTCC	ΔVC1807 F1 for UP arm
ABD340	gtcgacggatccccggaatACGTTTCATTAGTCACCTCTATTGTTAA CTTGTTC	ΔVC1807 R1 for Up arm
ABD341	gaagcagctccagcctacaTAGTCGAAAATAAAAAAAAGAGGCTC GCCTC	ΔVC1807 F2 for Down arm
BBC2412	CAATTTTGCTTTTGGACCATCC	ΔVC1807 R2 for Down arm
ABD725	GAAGCAGCTCCAGCCTACA	Detect F for all deletions
CKP001	cccgggatcctgtgtgaaattgCTTATTTGGCCTTGTTTGATAATG	ΔchiS detect R
CKP682	AATAGTCAACGTCAATTCTGTC	ΔtfoS detect R
BBC1786	TTTTGTGATGGCTGGATGTCG	ΔcrvA detect R
BBC030	ACCAAACAATAAACGAGTAATGC	ΔVC1807 detect R
Primers for Reporter Constructs		
Primer	**Sequence**	**Description**
BBC3230	GCAGTAAATCCGACTTTGGAG	Insert construct at igVCA0265-66 F1
BBC3260	CCCGGGATCCTGTGTGAAATTG	igVCA0265-66 $Spec^R$ R1 for P_{const2}
BBC4271	caatttcacacaggatcccgggAGGAGGTtGTGTTATGGTGAGCAAA GGTG	Amplify mTFP1 F
BBC4272	tgtaggctggagctgcttcCTATTTATACAGTTCATCCATACCATC	Amplify mTFP1 R
CKP803	gaagcagctccagcctacaTCATAATTTAAGGCGTTAGCAG	Insert construct at igVCA0265-66 F2
BBC3231	TCTCATAAACCTCATGGTAGACG	Insert construct at igVCA0265-66 R2

BBC832	GCTTTTTGCTACAACGACCG	Insert construct at VCA0692 F1
BBC263	TACCGAGGACGCGAAGCTGCTCATTAGGCACCCCAGGC	Insert construct at VCA0692 R1
CKP699	cagcttcgcgtcctcggtaAATAGTCAACGTCAATTCTGTC	Amplify PtfoR-GFP F
BBC254	tgtaggctggagctgcttcTTAGTTGTATAGTTCATCCATGCC	Amplify PtfoR-GFP R
BBC830	gaagcagctccagcctacaGTTGAGTTGGATGCAGCACC	Insert construct at VCA0692 F2
BBC834	CACAATTTCTCGCTTAAAATGTCC	Insert construct at VCA0692 R2
BBC2511	CTCATTAGGCACCCCAGGC	PtfoR$^{\Delta CBS}$-GFP R1
BBC4082	gcctggggtgcctaatgagTAAAATCAACACCTTAAAAACATGATTAAGC	PtfoR$^{\Delta CBS}$-GFP F2
VGP0466	tctctatcactgatagggaTAgAATAGGTACTAATCAgAATAGTGAGGAG	PtfoR$^{\Delta CBS::tetO}$-GFP R1
VGP0467	tccctatcagtgatagagaTCACATTACCATTAAgATGTCAAACGG	PtfoR$^{\Delta CBS::tetO}$-GFP F2
VGP0468	ctcctcactattctgattagtacctattctaTCCCTATCAGTGATAGAGAttcttTCCCTATCAGTGATAGAGAttcttTCCCTATCAGTGATAGAGAatcgtTCCCTATCAGTGATAGAGAtcacattaccattaagatgtcaaacgg	4X tetO miniFRT F
VGP0469	ccgtttgacatcttaatggtaatgtgaTCTCTATCACTGATAGGGAacgatTCTCTATCACTGATAGGGAaagaaTCTCTATCACTGATAGGGAaagaaTCTCTATCACTGATAGGGAtagaataggtactaatcagaatagtgaggag	4X tetO miniFRT R
BBC4945	TTTTCTGACTTGGTCTTTGACG	Insert X bp between CBS and TBS in PtoR-GFP R1
BBC4946	CGTCAAAGACCAAGTCAGAAAAtttttGTCTCCTGCATAAAATCAACATG	PtfoR^{+5}-GFP F2
BBC4947	CGTCAAAGACCAAGTCAGAAAAtttttttttGTCTCCTGCATAAAATCAACATG	PtfoR^{+10}-GFP F2
Primers for BACTH		
Primer	**Sequence**	**Description**
BBC2513	gaagcagctccagcctacaGATCCCCGGGTACCTAAGTAAC	Amplify BACTH pKT25 to make T25-XX vectors F
BBC2512	tccacctgctccacctgcCTCTAGAGTCGACCCTGCAG	Amplify BACTH pKT25 to make T25-XX vectors R
BBC2515	gaagcagctccagcctacaCCGAGCTCGAATTCATCGATATAAC	Amplify BACTH pUT18C to make T18-XX vectors F
BBC2514	tccacctgctccacctgcCTCTAGAGTCGACCTGCAG	Amplify BACTH pUT18C to make T18-XX vectors R
BBC2517	gcaggtggaagtggtggaGATCCCCGGGTACCGAGC	Amplify BACTH pKNT25 and pUT18 to make XX-T25 and XX-T18 vectors F
BBC2516	tccacctgctccacctgcCTCTAGAGTCGACCTGCAGG	Amplify BACTH pKNT25 and pUT18 to make XX-T25 and XX-T18 vectors R

BBC2762	gcaggtggagcaggtggaTTTAGGTTCTATCGAAAACAAAAATTC	BACTH TXX-ChiS or ChiS-TXX F
BBC3203	tgtaggctggagctgcttcTTATTCACTGGTCAGGAGTTTTTGC	BACTH TXX-ChiS R
BBC3204	tccaccacttccacctgcTTCACTGGTCAGGAGTTTTTGC	BACTH ChiS-TXX R
VGP0213	gcaggtggagcaggtggaTCGCTGACAGGGGAACTCG	BACTH TXX-TfoS or TfoS-TXX F
VGP0214	tgtaggctggagctgcttcTTAGTTTTCTTGATCTTCGATGAATTG	BACTH TXX-TfoS R
VEG0215	tccaccacttccacctgcGTTTTCTTGATCTTCGATGAATTGG	BACTH TfoS-TXX R
Primers for EMSAs		
Primer	**Sequence**	**Description**
BBC4084	gtcgacggatccccggaatCCGGTGATATTCTCATTTTAGC	P_{tfoR}^{WT} F from Fig. 1F
CKP235	gtcgacggatccccggaatCAAATATATCCTCCTCACTATTTTGATTAG	P_{tfoR}^{WT} and $P_{tfoR}^{\Delta CBS}$ F from Fig. S5
BBC929	AACATCACCATCTAATTCAACAAG	P_{tfoR}^{WT} and $P_{tfoR}^{\Delta CBS}$ R
CKP248	TGTACTGTACAAATATTTTTTTTGTACAG	$P_{VCA0053}$ F
CKP249	TGTGGGGTTGCCATGGTTAC	$P_{VCA0053}$ R
Primers for ChiS Constructs		
Primer	**Sequence**	**Description**
BBC4387	GATAACGATCGATAGCTGGTTGG	Insert construct at igVCA0587-88 F1
BBC647	tttttctatttctgaatcgattcatacgaCTCATTAGGCACCCCAGGC	igVCA0587-88 Erm^R R1
BBC1889	tcgtatgaatcgattcagaaatagaaaaaTTTGCCGCTTTTAACGTAAATCAG	Amplify PchiS-ChiS F
BBC577	tgtaggctggagctgcttcTTATTCACTGGTCAGGAGTTTTTGC	Amplify PchiS-ChiS R
BBC4384	gaagcagctccagcctacaGCAGTGTTGGCTGCAACTCC	Insert construct at igVCA0587-88 F2
BBC4388	ATCATGGTGCTGTTTAGTTGG	Insert construct at igVCA0587-88 R2
CAK311	ATTTTATGGCTGAATTTCATAATTAAGGTGTTACTTTCGGTG	Mlp37 periplasmic domain stitch to PchiS R1
CAK312	CCGAAAGTAACACCTTAATTATGAAATTCAGCCATAAAATTGTTG	Mlp37 periplasmic domain stitch to PchiS F
CKP384	GCGGTGAGGTAATGAAATTAACGATAAACAGTAGAACAAACACG	Mlp37 periplasmic domain R
CKP385	TTCTACTGTTTATCGTTAATTTCATTACCTCACCGCTTTTG	ChiS HAMP + cytoplasmic stitch to Mlp37 periplasmic F2
CKP397	ataatcaatgtcgtgatccttgtagtcaccatcatggtctttataatcATCGACAATCTCATCAACACTG	Mlp37 periplasmic domain truncation 3X FLAG R1
CKP396	ggtgactacaaggatcacgacattgattataaggatgacgatgacaaaGAATTTTTGGGTGAAAGCAAAATC	Mlp37 periplasmic domain truncation 3X FLAG F2
BBC4756	gccagctttcgcggcagcttcgccaccagaaccgctTTGATACTCGCCCGAGGCTT	Amplify $ChiS^{\Delta DBD}$ R1
BBC4757	agcggttctggtggcgaagctgccgcgaaagctggcGTGTCTAGATTAGATAAAAGTAAAGTG	Amplify TetR F
VGP0470	tgtaggctggagctgcttcTTAtccacctgctccacctgc	Amplify TetR R

Primers for POLAR Constructs		
Primer	**Sequence**	**Description**
ABD332	GGCTGAACGTGGTTGTCGAAAATGAC	Insert construct at *lacZ* F1
BBC3668	cagctttcgcggcagcttcgccaccagaaccgctGTTTTCTTGATCTTCGATGAATTGGC	Amplify TfoS R1
BBC3669	ttctggtggcgaagctgccgcgaaagctggcGTGagcaagggcgaggaggataacatgg	Amplify mCherry F
BBC206	tgtaggctggagctgcttcttacttgtacagctcgtccatg	Amplify mCherry R
ABD255	gaagcagctccagcctacaCCACAATAAGCCAGAGAGCCTTAAG	Insert construct at *lacZ* F2
ABD256	CCCAAATACGGCAACTTGGCG	Insert construct at *lacZ* R2
Primers for TfoS Constructs		
Primer	**Sequence**	**Description**
ABD332	GGCTGAACGTGGTTGTCGAAAATGAC	Insert construct at *lacZ* F1
BBC244	CCCGGGATCCTGTGTGAAATTGTTATCCGC	Insert construct at *lacZ* Zeo^R R1
BBC4343	caatttcacacaggatcccgggAGGAGGTGAACTCaTGTTTCGCACATTG	Amplify TfoS for Ptac F
BBC2476	tgtaggctggagctgcttcTTAGTTTTCTTGATCTTCGATGAATTGGC	Amplify TfoS for Ptac R
ABD255	gaagcagctccagcctacaCCACAATAAGCCAGAGAGCCTTAAG	Insert construct at *lacZ* F2
ABD256	CCCAAATACGGCAACTTGGCG	Insert construct at *lacZ* R2
ABD640	GCAATACACGCTGTGTTTCACCG	Amplify native TfoS F1
CKP760	tccaccacttccacctgcATTTCTCACTTCAAGTTGTATGG	Insert tag after TfoS N929 R1
BBC2274	gcaggtggaagtggtggagattataaggatgacgatgacaaagcaggtggagcaggtgga	1X FLAG F
BBC2275	tccacctgctccacctgctttgtcatcgtcatccttataatctccaccacttccacctgc	1X FLAG R
CKP761	gcaggtggagcaggtggaGCGCAGGCGGTTATCGTATTTTC	Insert tag after TfoS N929 F2
ABD643	TCGTTTTCTAAGGCTCGAATCGCC	Amplify native TfoS R2
Primers for TfoR Constructs		
Primer	**Sequence**	**Description**
BBC4983	GTGATACCACAAGCAACTATACC	TfoR F1
BBC4980	gcttaatcatgtttttaaggtgttgattttaACCTAAGCAAACATTGTTTTCG	Delete CBS in PtfoR R1
BBC4981	cgaaaacaatgtttgcttaggtTAAAATCAACACCTTAAAAACATGATTAAGC	Delete CBS in PtfoR F2
BBC4984	TCGTGCAACTTGAGAGTAACAAC	TfoR R2
VGP0478	tagaataggtactaatcagaatagtgaggagACCTAAGCAAACATTGTTTTCG	Insert 4X tetO in PtfoR R1
VGP0480	CTCCTCACTATTcTGATTAGTACC	Amplify 4X tetO F
BBC4338	CTCATTAGGCACtCCAGGC	Amplify 4X tetO R
VGP0479	gcctggagtgcctaatgagTAAAATCAACACCTTAAAAACATGATTAAGC	Insert 4X tetO in PtfoR F2
BBC706	CCACACATTATACGAGCCGATG	Amplify TfoR for Ptac R1

BBC708	CATCGGCTCGTATAATGTGTGGATTCCAGAGGTGGTATGACC	Amplify TfoR for Ptac F2

994